Ground state and quasi-γ bands in the even Ba chain

A. Giannatiempo

Dipartimento di Fisica e Astronomia, Università di Firenze, IT-50019 Sesto Fiorentino (Firenze), Italy

The ground state band of the even $^{118-134}$Ba and $^{142-150}$Ba isotopes, which extend over two neutron major shells, and the quasi-γ band, in the neutron-deficient Ba region, have been investigated in the framework of the IBA-2 model. All available spectroscopic data concerning these isotopes have been compared to the calculated values. It has been found that the two bands have different symmetry in the proton and neutron degrees of freedom. Their structure evolution, as a function of the neutron number, and the decay properties of the quasi-γ band have been studied in detail.

I. INTRODUCTION

The $Z \simeq 56$ even isotopic chains extend over the [50–82] and [82–126] neutron major shells. A first indication of the dramatic change in the structure of these isotopic chains, in going from the neutron-deficient to the neutron-rich region, stems from Fig. 1. Here, the excitation energy ratio of the 4_1^+ to the 2_1^+ state, $R_{4/2}$, for the even $Z = 52$–60 isotopic chains, is reported as a function of the neutron number, N.

As is well known, the $R_{4/2}$ ratio is one of the most important structural signatures, the larger its value, the stronger the deformation. In the $N < 82$ region, the relevant isotopic chains display strongly different $R_{4/2}$ patterns, as a function of N. In the even Te and Xe isotopic chains, effects related to the underlying nuclear structure are clearly apparent. For $Z \geqslant 56$, the isotopic chains have mainly collective nature (apart from a small region around $N = 82$), as revealed by the $R_{4/2}$ monotonic increase in approaching the neutron midshell ($N \simeq 66$). Only for $Z \geqslant 58$ the deformation attains a value close to that of a well-deformed nucleus ($R = 3.3$), whereas, for $Z = 56$, it is still remarkably lower ($R \simeq 2.9$). In the $N > 82$ region, for $Z \geqslant 54$ the transition from a spherical to a deformed shape is sharp, with $R_{4/2}$ slopes rather similar for the different isotopic chains. In Fig. 1, two dashed vertical lines, drawn for a neutron number differing by ± 10 from $N = 82$, help highlighting the different increase of deformation in the relevant isotopic chains, when moving away from the $N = 82$ shell closure.

The description of low-lying collective excitations in an isotopic chain developing along two neutron major shells, with strong structural changes, is a difficult task. To approach this problem the interacting boson approximation (IBA) model [1] is particularly suitable. In this model, based on a group-theoretical description of collective quadrupole excitations in nuclei, the boson are identified as correlated pairs of like nucleons moving in a valence space. The IBA-1 version of the model predicts groups of states fully symmetric (FS) in the degrees of freedom of protons and neutrons. Its U(5), O(6), and SU(3) symmetry limits correspond, in

a geometrical model, to the harmonic vibrators, γ-unstable, and symmetrically deformed nuclei, respectively. The model space is significantly extended in the IBA-2 version of the model, where valence protons and neutrons are separately considered. In fact, in addition to FS states, it predicts the existence of new groups of states, the so-called mixed symmetry (MS) states [2–4], which contain antisymmetric combinations of neutron and proton bosons. As far as only FS states are concerned, the $U_{\pi,\nu}(5)$, $O_{\pi,\nu}(6)$, and $SU_{\pi,\nu}(3)$ limits of the IBA-2 version correspond to the U(5), O(6), and SU(3) limits of the IBA-1 version. The importance of MS states in determining the structure of even-even nuclei at low energy, in different mass regions, has become increasingly evident over the years (see, e.g., Refs. [5–14]).

In the study of an isotopic chain, the identification of nuclei close to the X(5) [15] critical point symmetry can help to investigate the structure evolution. This dynamical symmetry, which corresponds to an analytic solution of a simplified Bohr Hamiltonian, describes nuclei near the critical point of a spherical to axially symmetric rotor shape transition, which corresponds to an U(5) to SU(3) transition.

The study of the even Ba chain, in the framework of the IBA model, has extended over the decades (see, e.g., Refs. [16–30]), exploiting the new available information. It was early found that $^{128-134}$Ba isotopes display properties consistent with the O(6) limit [18] and since the very beginning it has been widely thought that the structure of the isotopic chain in the $N < 82$ region changes gradually from a γ-soft to an axially symmetric one, as N approaches the neutron mid shell. In a different interpretation proposed by Zamfir *et al.* [31], in reality, the O(6) symmetry would be an intermediate structure situated on a U(5) to SU(3) transitional region. As to the MS states in the even Ba chain, their presence has been proposed or recognized in some of the $N < 82$ Ba isotopes, limited to the lowest 1^+ and 2^+ states (see, e.g., Refs. [6,26,32,33]), while, to my knowledge, no MS state has been identified in the neutron-rich Ba isotopes.
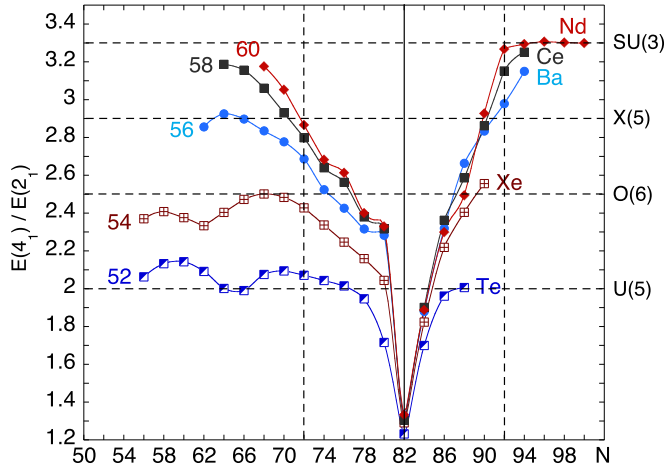
FIG. 1. Excitation energy ratios, $R_{4/2}$, of the 4_1^+ to the 2_1^+ state in the even $Z = 52$–60 isotopic chains. The atomic number is reported next to each isotopic chain. Horizontal lines indicate the $R_{4/2}$ value of the U(5), O(6), and SU(3) limits of the IBA model and of X(5) dynamical symmetry. The vertical continuous line marks the $N = 82$ shell closure. Two vertical dashed lines are drawn at $N = 72$ and $N = 92$ (see text for details).

The aim of the present work is to study the structure of the g.s. band in the even $^{118-134}$Ba and $^{142-150}$Ba isotopes and of the quasi-γ bands in the even $^{122-134}$Ba isotopes. The g.s. band, which approaches the proton-drip line on the neutron-deficient side and extends 12 isotopes away from the most abundant one on the neutron-rich side, has a widely different nuclear deformation trend in the two neutron major shells. The description of such characteristics, possibly with a limited number of parameters, is the first goal of the present work.

The second one is to extend to the $A \simeq 130$ mass region the search of a possible coexistence of a g.s. band of FS character and a quasi-γ band of MS character, a phenomenon already pointed out in the $A \simeq 80$ [5] and $A \simeq 110$ [34,35] mass regions. For simplicity, from now on only the term γ band is used, even though the term quasi-γ band would be more appropriate.

II. IBA-2 ANALYSIS AND RESULTS

The chain of the Ba isotopes, in which excited states have been observed, extends from $A = 118$ to $A = 150$. The ^{138}Ba ($N = 82$) isotope has been obviously excluded from the present study, as have been the neighboring ^{136,140}Ba, where collective bands are not observed.

As to the g.s. band, the limit $J \leqslant 10$ on the spins taken into account is due to back-banding effects, which show up when the yrast band extends to higher J values. In ^{132}Ba the g.s. band has been observed only up to $J = 8$. In ^{134}Ba two states having $J^\pi = (6^+)$ and a (8^+) have been reported in Ref. [36] as members of the g.s. band. However, the energy spacing of the $(8^+) \rightarrow (6^+) \rightarrow 4^+$ cascade does not correspond to that typical of a collective band, where two subsequent transitions have an energy ratio >1, increasing with J, so that they have been excluded from the analysis. The excitation energy ratios
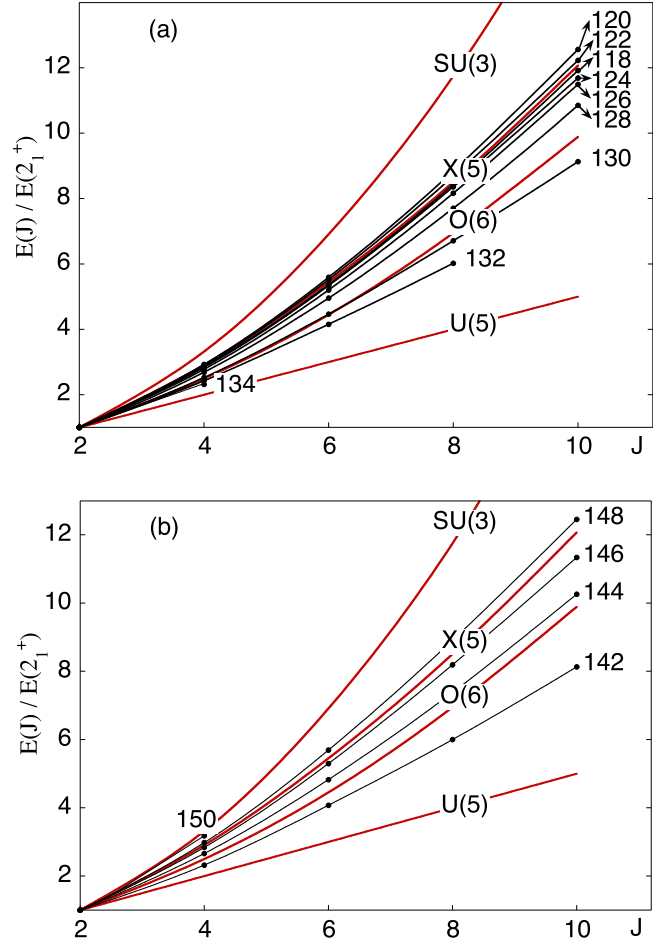

FIG. 2. Excitation energies of the g.s. states, relative to that of the 2_1^+ state, as a function of J, for: (a) $^{118-134}$Ba, (b) $^{142-150}$Ba. The corresponding predictions of the U(5), O(6), and SU(3) limits are also reported, together with those of the X(5) critical point symmetry.

of all the states taken into account in the present study to that of the 2_1^+ state, $R_{J/2}$, are shown, as a function of J, in Fig. 2.

As to the γ band, it has been observed in the even $^{122-134}$Ba isotopes. In ^{132}Ba a $6^{(+)}$ state at 2241 keV, reported in Ref. [37] as a member of the γ band, has been disregarded because the $6^{(+)} \rightarrow 4_2^+$ transition energy (511 keV) is definitely smaller than that (626 keV) of the $4_2^+ \rightarrow 2_2^+$ transition.

Very recently Naïdia *et al.* [38] have found a band in ^{142}Ba they identify as the γ band, even though it appears to be quite different from those observed in the lighter isotopes. From Fig. 2(b), it is seen that the g.s. band of this isotope lays in a region between the U(5) and O(6) limits, not far from the O(6) one. It is almost the same region where the g.s. band of ^{130}Ba is positioned in Fig. 2(a). The excitation energy trend, as a function of J, of the g.s. and γ bands of the two isotopes are compared in Fig. 3. The g.s. bands have a very similar behavior, so that it seems reasonable to expect that this is also the case for the γ bands. Instead, in ^{130}Ba the 2^+ band head has quite the same excitation energy as the 4_1^+ state, whereas in ^{142}Ba it is very close to the 6_1^+ state. This is not in agreement with what is predicted by both U(5) and O(6) limits, i.e., that
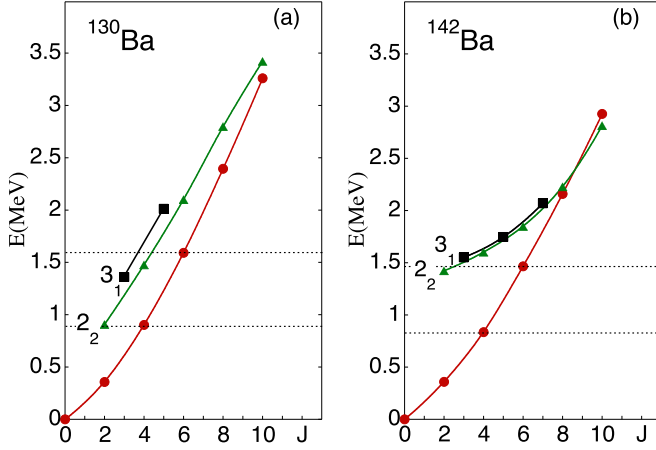
FIG. 3. Excitation energies of the g.s. and γ bands in (a) ^{130}Ba, and (b) ^{142}Ba isotopes. Two different lines connect the even-spin (triangles) and the odd-spin (squares) states of the γ bands. The horizontal lines mark the excitation energies of the 4_1^+ and 6_1^+ states in the two isotopes.

the band head of the γ band is the 2_2^+ state, degenerate in energy with the 4_1^+ state. Further, the slope of the γ band in ^{142}Ba, as a function of J, is completely different from that observed in ^{130}Ba, which is similar to that in ^{132}Ba. Therefore, such a band has been excluded from the present study.

In the analysis of the levels of interest in the even $^{118-134,142-150}$Ba isotopes all available excitation energies and electromagnetic (e.m.) properties have been considered. The experimental values are taken from Ref. [39], unless explicitly mentioned otherwise.

The Hamiltonian utilized in the present work reads

$$H = \varepsilon \left(\hat{n}_{d_\pi} + \hat{n}_{d_\nu} \right) + \kappa \, \hat{Q}_\pi^{(\chi_\pi)} \cdot \hat{Q}_\nu^{(\chi_\nu)} + \hat{M}_{\pi\nu}[\xi_1, \xi_2, \xi_3], \quad (1)$$

where

$$\hat{Q}_\rho = (d_\rho^\dagger \times \tilde{s}_\rho + s_\rho^\dagger \times \tilde{d}_\rho)^{(2)} + \chi_\rho (d_\rho^\dagger \times \tilde{d}_\rho)^{(2)}. \quad (2)$$

The indexes π and ν refer to proton and neutron bosons, respectively. In Eq. (1) the first term represents the d-boson energy; $\hat{n}_d$ ($\hat{n}_d = \hat{n}_{d_\pi} + \hat{n}_{d_\nu}$) is the d-boson number operator. The second term represents the quadrupole interaction and the third one the Majorana operator [40], which has nonzero eigenvalues only for MS states. This last property provides a first hint for the presence of important MS components in the structure of the states. The Majorana parameters ξ_1, ξ_2, ξ_3 can take independent values [41–44].

In the IBA-2 model the $E2$ and $M1$ operators are expressed as [1]

$$\hat{T}(E2) \equiv e_\nu \, \hat{T}_\nu(E2) + e_\pi \, \hat{T}_\pi(E2)$$
$$= e_\nu \, \hat{Q}_\nu(E2) + e_\pi \, \hat{Q}_\pi(E2), \quad (3)$$
$$\hat{T}(M1) \equiv g_\nu \, \hat{T}_\nu(M1) + g_\pi \, \hat{T}_\pi(M1)$$
$$= \sqrt{\frac{30}{4\pi}} [g_\nu (d_\nu^\dagger \times \tilde{d}_\nu)^{(1)} + g_\pi (d_\pi^\dagger \times \tilde{d}_\pi)^{(1)}], \quad (4)$$

where e_ρ and g_ρ ($\rho = \pi, \nu$) are the effective quadrupole charges and gyromagnetic ratios, respectively. The values of

χ_ρ are the same as in the Hamiltonian (consistent-Q formalism [45]). Because of the form of the transition operators, $E2$ transitions obey the selection rule $\Delta n_d = 0, \pm 1$ while $M1$ transitions can only connect states having the same d-boson number. The reduced matrix elements $\langle \|\hat{T}_\nu\| \rangle$ and $\langle \|\hat{T}_\pi\| \rangle$ of the $M1$ transition operator have always the same absolute values but opposite signs [32,46], so that $M1$ transition probabilities are proportional to $(g_\pi - g_\nu)^2$.

The numerical diagonalization of the Hamiltonian has been performed in the $U_{\pi,\nu}(5)$ basis, using the NPBOS code [47]. It gives, as outputs, the d-boson number and F-spin components of each wave function. The F-spin quantifies the symmetry of a state in the proton and neutron degrees of freedom. Analogously to the fermionic isospin, it has projection $F_z = +1/2$ for proton and $F_z = -1/2$ for neutron bosons. In the limits of the model, where the F-spin is a good quantum number, FS states have eigenvalue $F = F_{\max} = 1/2 (N_\pi + N_\nu)$, where N_π and N_ν are the proton and neutron boson numbers, respectively. Mixed symmetry, MS, states are characterized by $F = F_{\max} - 1, F_{\max} - 2 \ldots$, down to the minimum value $F_{\min} = 1/2 |N_\pi - N_\nu|$. The bosons are counted with respect to the nearest closed shell, as particles from the beginning of the shell up to the midshell and as holes in the second half of the shell.

Both $E2$ and $M1$ transitions satisfy the F-spin selection rule, $\Delta F = 0, \pm 1$. In addition, $M1$ transitions are forbidden between FS states [32,46]. Such a property has been always exploited as an outstanding signature for states having large MS components.

The Hamiltonian parameters have been deduced via an iterative procedure. Initial values, deduced through a comparisons of the excitation energies, were modified to reproduce, as closely as possible, the e.m. properties of the relevant isotopes, to be again compared to the excitation energies and so on, until satisfactory convergence to final values was obtained. The final determination of χ_π and χ_ν, which affect both excitation energies and transition strengths, has been made difficult by the lack of definite information on the quadrupole moments. Therefore, for these parameters some support was obtained by taking into account some general properties considered in microscopic models [48]: (i) χ_π depend only on N_π and χ_ν on N_ν; (ii) they both assume high, negative values at the beginning of a major shell and increase their values, as a function of N_π or N_ν, respectively, up to achieving high, positive values approaching the major shell closure. As to the choice of a fixed value for χ_π, two possible values have been considered, -0.5 and -1.0, finding that the latter leads to a better agreement with the experimental data.

For what concerns the Majorana parameters, it has been found in previous works (see, e.g., Refs. [5,12,43]) and further checked in the present one, that the calculated excitation energies of the g.s and γ bands are basically independent of ξ_1. Its value has been arbitrarily kept to 1 MeV. It has been also checked that the excitation energies of the g.s. band are essentially not influenced by the ξ_2 and ξ_3 values. Therefore, for those isotopes in which only a g.s. band has been established, the value of these parameters have been kept fixed at 1 MeV. The full set of the Hamiltonian parameters eventually adopted is reported in Table I.

TABLE I. Adopted values for the Hamiltonian parameters used in IBA-2 calculations. All parameters are given in MeV, apart from χ_ν (dimensionless). The value $\chi_\pi = -1.0$ has been adopted for all isotopes. The ξ_1 parameter has been fixed at 1 MeV. The ξ_2 and ξ_3 values are reported in italics whenever arbitrarily fixed at 1 MeV (see text for details).

A	ϵ	κ	χ_ν	ξ_2	ξ_3
118	0.650	−0.110	−0.800	*1.0*	*1.0*
120	0.660	−0.120	−0.500	*1.0*	*1.0*
122	0.660	−0.120	−0.400	−0.090	−0.100
124	0.660	−0.140	0.100	−0.100	−0.080
126	0.660	−0.140	0.100	−0.110	0.000
128	0.660	−0.140	0.100	−0.100	0.100
130	0.700	−0.140	0.100	−0.100	0.000
132	0.780	−0.170	0.300	−0.060	−0.100
134	0.880	−0.200	0.800	0.030	−0.220
142	0.580	−0.085	−1.100	*1.0*	*1.0*
144	0.445	−0.080	−0.900	*1.0*	*1.0*
146	0.470	−0.080	−0.800	*1.0*	*1.0*
148	0.440	−0.080	−0.700	*1.0*	*1.0*
150	0.310	−0.135	−0.600	*1.0*	*1.0*

An example of the role played by ξ_2 and ξ_3 when attempting to reproduce the excitation energies of the γ bands is shown in Fig. 4. Here, the experimental excitation energies of the odd-spin members of the band in $^{122-128}$Ba are compared with those calculated using the adopted set of parameters reported in Table I or by choosing $\xi_2 = \xi_3 = 1$ MeV. With the latter choice, the calculated states have an $F_{\max}$ component (amplitude square) larger than 0.98, since all MS states have been moved to much higher energies, and no agreement with the experimental data would be obtained.

As to the e.m. parameters, the effective boson charges have been kept fixed to the values $e_\pi = 0.15$ e b, $e_\nu = 0.12$ e b and the gyromagnetic factors to $g_\pi = 0.43\,\mu_N$, $g_\nu = 0.28\,\mu_N$. The value of g_ν is equal to that adopted in Refs. [12,43] for the even Pd chain and in Ref. [34] for the even Ru chains. The value of g_π is slightly smaller than that (0.51 μ_N) used in the same references for both isotopic chains. The values of the gyromagnetic ratios affect drastically all $M1$ transition strength, which, as mentioned above, are proportional to $(g_\pi - g_\nu)^2$.

It is to be remarked that different parameter sets can lead to comparable excitation energy patterns, but that this is not the case when the e.m. properties are concerned.

The comparison of the available electric quadrupole moments, $Q(J)$, and magnetic moments, $\mu(J)$, with the calculated values is reported in Table II. Only two quadrupole moments have been measured and, in both cases, two conflicting experimental data are found in the literature. A first idea of capability of the model to reproduce the experimental data along the [50–82] and [82–126] neutron shells, as far as the excitation energies are concerned, can be obtained from Fig. 5. As to $N < 82$ isotopes, experimental and calculated decay patterns concerning the g.s. and the γ bands are shown in Figs. 6–10.

In ^{118,120}Ba, where only the excitation energies are known, the detailed comparison shown in Fig. 6 makes it possible to
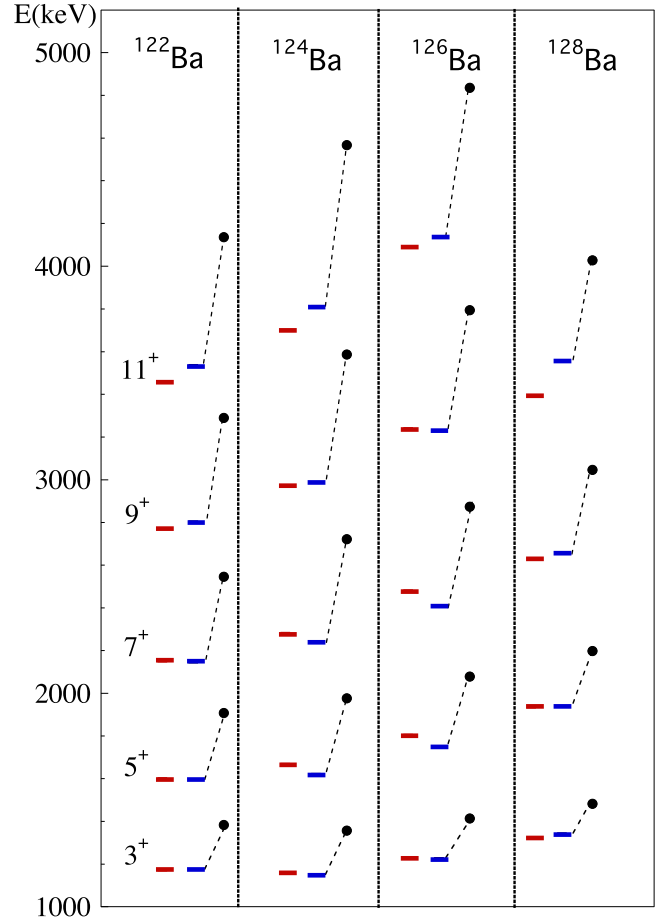

FIG. 4. The experimental (red line on the left) excitation energies of the odd spin states of the γ band in $^{122-128}$Ba isotopes are compared to those calculated (blue line on the right) with the parameters reported in Table I and keeping the values of the Majorana parameters at 1 MeV (closed circles).

perceive its goodness (better than 0.1%, on the average). Due to the closeness of these isotopes to the proton drip line, such a result is of particular interest. Indeed, it assures the validity of the shell model (which is at the basis of the IBA model) even when the neutron-deficient Ba isotopes approach the extreme limit of the stability valley.

The experimental $B(M1)$ and $B(E2)$ transition strengths are compared with the calculated ones in Table III and IV, respectively. The two values reported for both the measured

TABLE II. Experimental electric quadrupole moments (in e b) and magnetic dipole moments (in μ_ν units) are compared to the calculated ones (in italics).

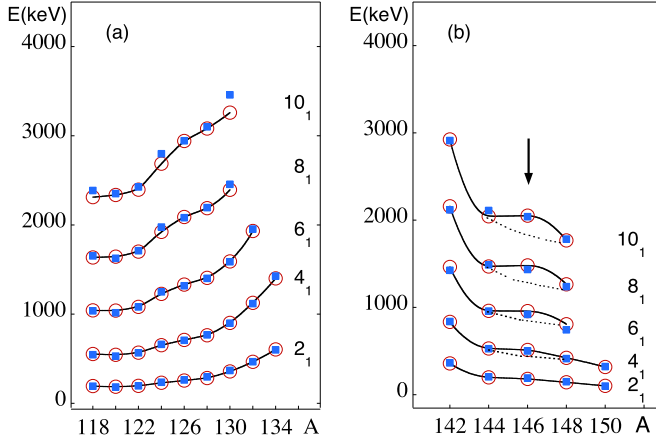| A	$Q(2_1^+)^{\text{exp}}$	$Q(2_1^+)^{\text{calc}}$	$\mu(2_1^+)^{\text{exp}}$	$\mu(2_1^+)^{\text{calc}}$
130	−1.02(16) or −0.09(16)	−0.73	0.70(6)	0.73
132			0.68(6)	0.73
134	−0.26(8) or +0.15(8)	−0.14	0.84(10)	0.74
142			0.85(10)	0.74
144			0.68(10)	0.71
146			0.52(10)	0.69

FIG. 5. Experimental (circles) and calculated (squares) excitation energies of the g.s. bands of the relevant (a) neutron-deficient and (b) neutron reach Ba isotopes. A line connects the experimental data. In (b) the expected trend for a regular deformation increase is shown by a dashed line; an arrow points out the presence of the $2\nu f_{7/2}$ subshell closure.

$B(E2; 8_1^+ \rightarrow 6_1^+)$ and $B(E2; 10_1^+ \rightarrow 8_1^+)$ values in ^{126}Ba are incompatible. In going from ^{128}Ba to ^{134}Ba the experimental $B(E2; 2_1^+ \rightarrow 0_1^+)$ transition strength smoothly reduces. It is not so for the experimental $B(E2; 2_2^+ \rightarrow 2_1^+)/B(E2; 2_2^+ \rightarrow 0_1^+)$ ratios, whose value in ^{132}Ba (3.3) largely exceeds those in the neighboring ^{128}Ba (0.45) and ^{134}Ba (2.2) isotopes. This suggests possible problems in the measurement.

The experimental mixing ratios [$\delta(E2/M1)$] are reported with the calculated absolute values In Table V. Next to each predicted value is shown the corresponding percentage of $M1$ component, obtained from the expression

$$W_\gamma(M1)/[(W_\gamma(M1) + W_\gamma(E2))] = 1/(1 + \delta^2). \quad (5)$$

Here, W_γ is the usual γ transition probability for the indicated multipolarity.

The impossibility of a comparison including a sign of δ arises from the fact that, in the majority of cases, the mix-
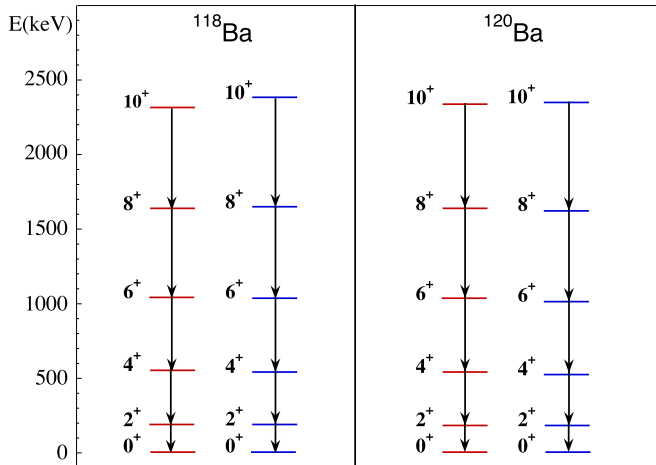
ing ratios have been deduced from $\gamma - \gamma$ angular-correlation measurements. In the literature, there are different definitions for A_{kk}, the most popular of which are those of Krane and Steffen [63] and Frauenfelder and Steffen [64], which lead to a different δ sign. Unfortunately, some authors do not mention the convention used in extracting the mixing ratio from the experimental data, which is the reason for limiting the comparison to absolute values.

It is worth mentioning that the 0_2^+ states, band heads of the so-called β bands, have been observed in the even $^{124-132}$Ba isotopes and that the calculations reasonably reproduce their excitation energies (see Table VI) without any *ad hoc* tuning of the parameters. However, the lack of experimental data does not allow one to extend to the β bands the study of the low-lying bands in the light Ba isotopes. As to the $N > 82$ isotopes, the experimental data concerning excitation energies and $B(E2)$ transition strengths of the g.s. band are reported in Fig. 11, where they are compared to the predicted values.

To summarize the results:

  (i) On the average, the calculations reproduce the excitation energies of the g.s. band and of the γ band better than 1%. In the $N > 82$ isotopes effects due to the presence of a partial subshell closure at $N \simeq 90$ (see Fig. 5) are well matched.

 (ii) The very limited information on the quadrupole moments is of great drawback to the whole analysis.

(iii) The magnetic moments are correctly reproduced.

 (iv) Only seven $B(M1)$ transitions strengths are known. Their order of magnitude, which ranges from $10^{-5} \mu_N^2$ to $10^{-3} \mu_N^2$, is reproduced in five cases out of seven.

  (v) In most cases the agreement between the calculated $B(E2)$ transition strengths and the experimental values is within 1, 2 standard deviations. It is to be remarked that in the $N < 82$ isotopes the $B(E2)$ values span three orders of magnitude.

 (vi) A striking feature of the decay of the $N < 82$ Ba isotopes is the large number of transitions having not negligible or large $M1$ components. The order of magnitude of the mixing ratios is reasonably reproduced.

(vii) As to the branching ratios, the overall experiment-theory agreement is satisfactory, apart from that concerning the 4_2^+ level in ^{134}Ba. Since in this isotope also the $B(M1; 4_2^+ \rightarrow 4_1^+)$ value is largely overestimated, the possibility of considering the 4_2^+ state as belonging to the IBA-2 model space is doubtful.

(viii) On the whole, the trend of the excitation energies and the $E2$ reduced transition strengths of the g.s. band in the $N > 82$ isotopes are correctly matched.

FIG. 6. Experimental (left) and calculated (right) decay pattern of the g.s. band of ^{118}Ba and ^{120}Ba.

III. DISCUSSION

From the analysis reported in Sec. II it appears that, on the whole, the properties of the g.s. and γ bands are satisfactory
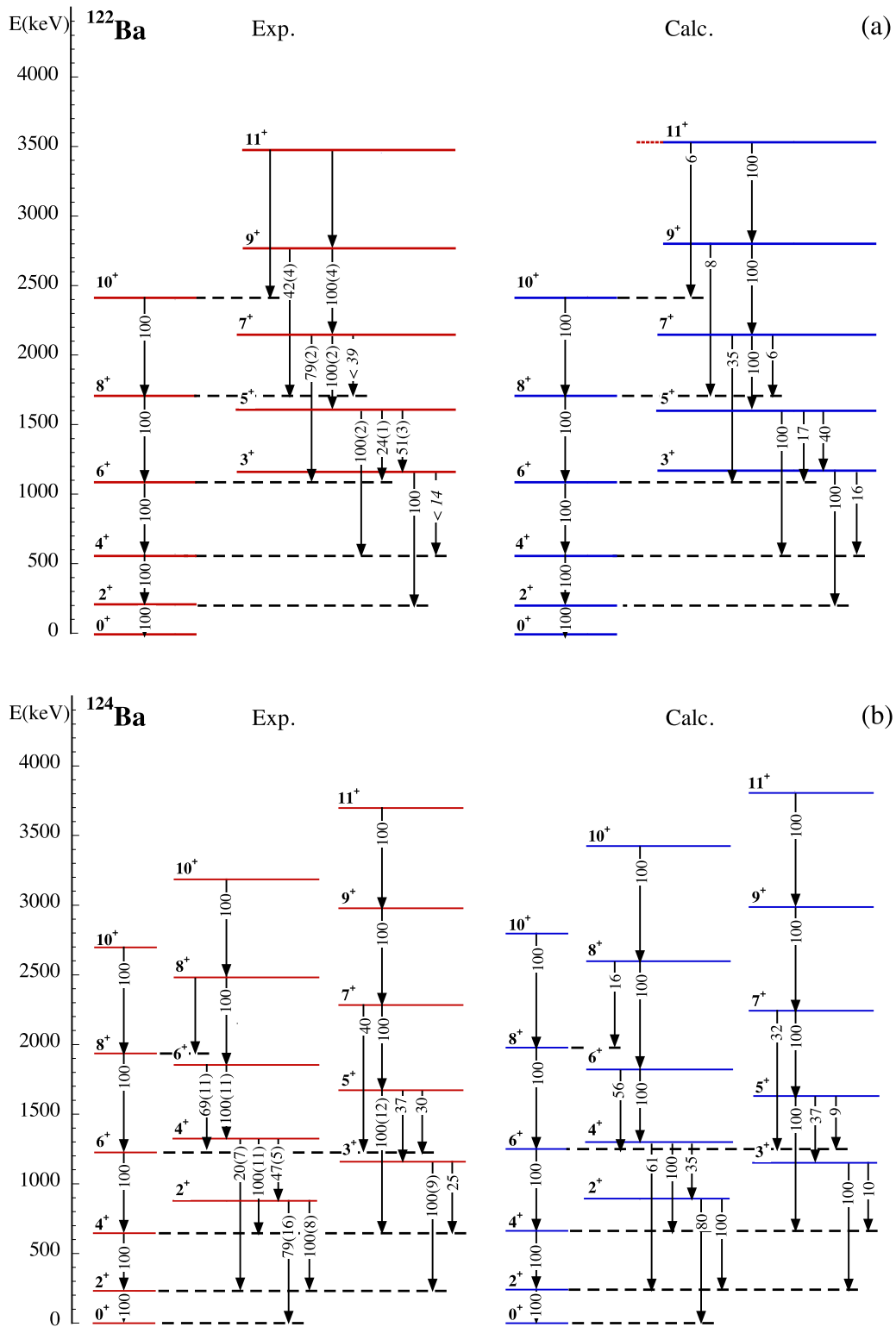
FIG. 7. Experimental and calculated decay patterns of (a) ^{122}Ba and (b) ^{124}Ba. In ^{122}Ba two experimental intensity ratio values, given as doubtful in Ref. [49], are reported in italics. In ^{124}Ba the $8_2^+ \rightarrow 8_1^+$ transition has been observed only as a part of an unresolved doublet [50], so that its intensity relative to the $8_2^+ \rightarrow 6_2^+$ transitions is unknown.

reproduced. These results suggest performing a detailed analysis of the relevant wave functions, starting with a preliminary description of the $U_{\pi,\nu}(5)$ basis states, on which they are expanded.

According to the F-spin and n_d quantum numbers, the $U_{\pi,\nu}(5)$ basis states can be arranged in groups, whose excitation energies have different dependence on the Majorana parameters [42–44]. A partial excitation pattern of
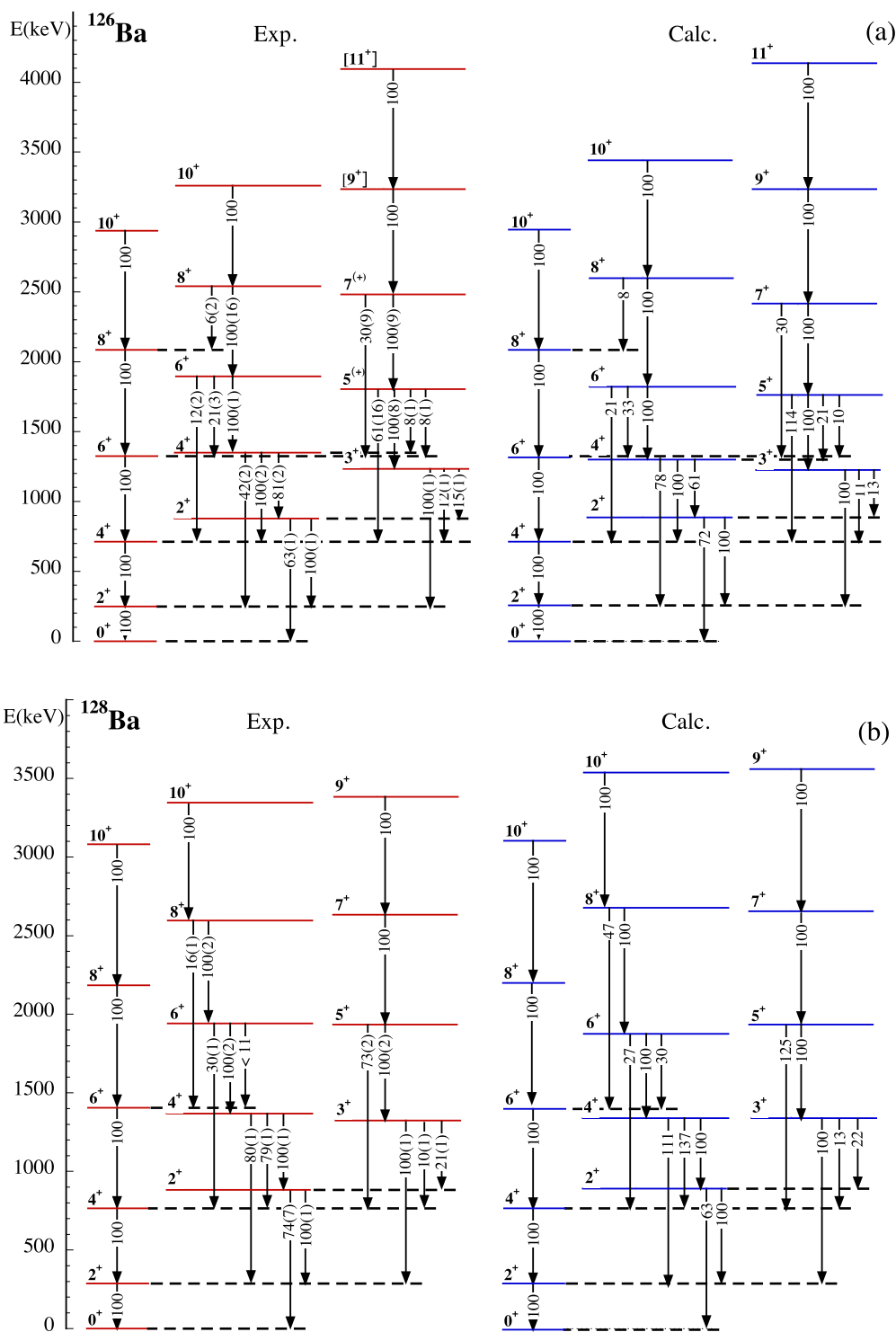
FIG. 8. Experimental and calculated decay pattern of (a) ^{126}Ba and (b) ^{128}Ba.

a $U_{\pi,\nu}(5)$ nucleus, having $N_\pi = 3$ (as the Ba chain) and $N_\nu = 4$, is shown in Fig. 12. The states included in frame [Fig. 12(b)] are members of the γ band in the IBA-1 model. The states in frame [Fig. 12(c)] are the counterpart of the states in frame [Fig. 12(a)], that is, have the same structure but a lower degree of symmetry, whereas the states in frame [Fig. 12(d)] do not have corresponding FS states.

As to the realistic wave functions of the relevant states in the $N < 82$ isotopes, the amplitude square of the F-spin components are reported in Figs. 13 and 14, those of the n_d components in Figs. 15 and 16, separately for the g.s. band and for the even- and odd-spin branches of the γ band. For ^{118,120}Ba and for the $N > 82$ isotopes the F-spin components are not shown because the high values adopted for the Majorana parameters lead to a percentage of the $F_{\max}$ components
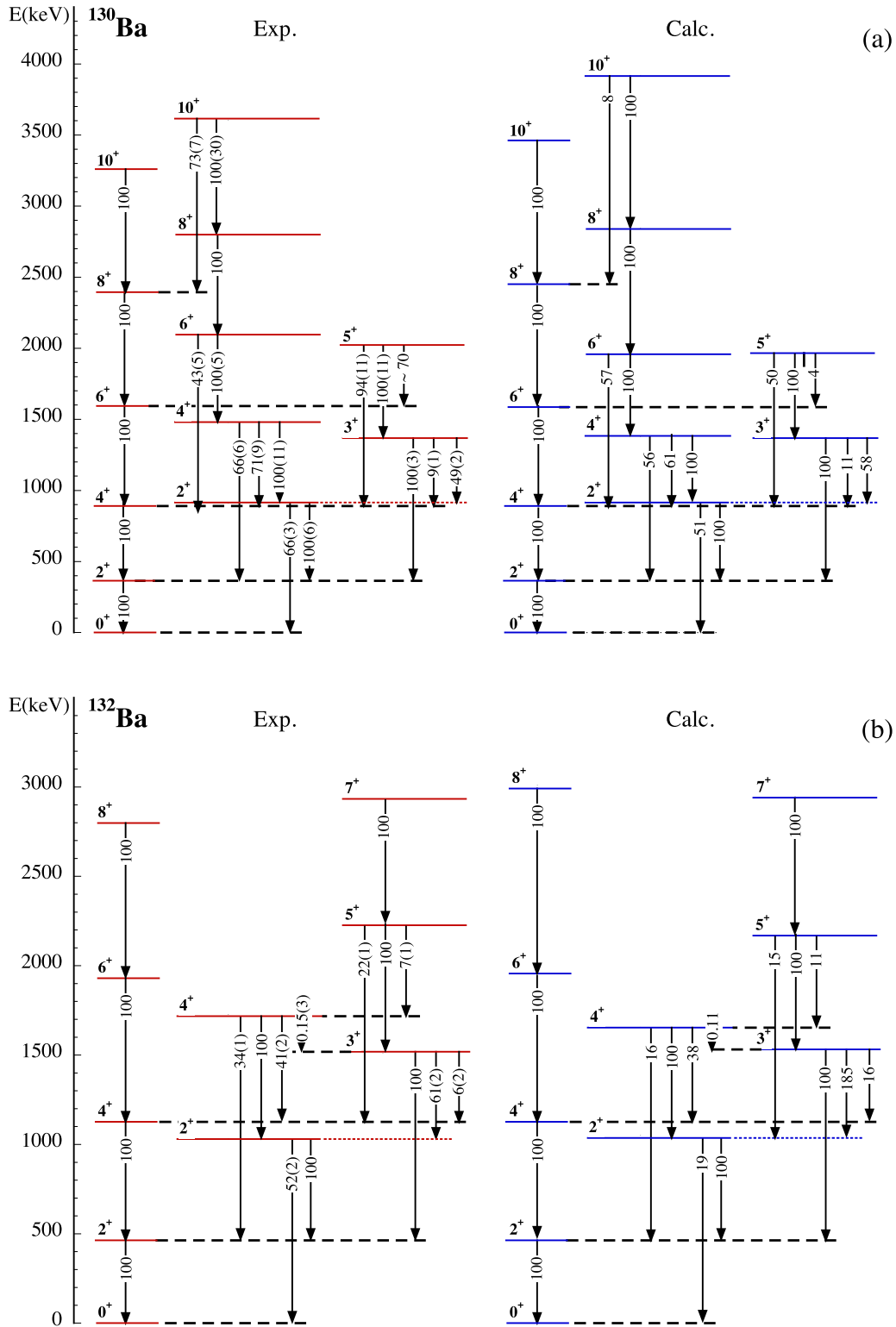
FIG. 9. As Fig. 8, for (a) ^{130}Ba and (b) ^{132}Ba.

close to 100%. The n_d components of the $N > 82$ isotopes are displayed in Fig. 17.

Joining the information provided by the F-spin and n_d components of the relevant states, it is possible to investigate the structure evolution of the Ba isotopes, as a function of N.

A. Structure evolution of the g.s. band in neutron-deficient and neutron-rich Ba isotopes

To study the evolution of the g.s. band along the [50–82] and [82–126] neutron major shells, it is useful to compare the structure of each state of the relevant isotopes with that
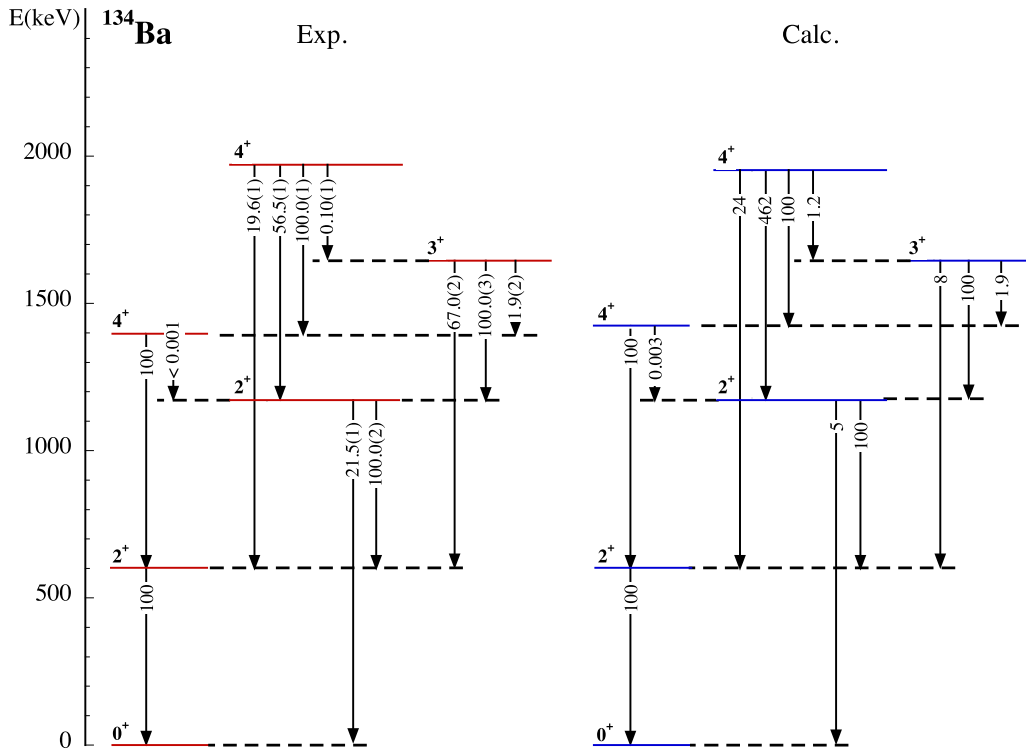
FIG. 10. As Fig. 8, for ^{134}Ba.

of the state of same J in the $U_{\pi,\nu}(5)$, $O_{\pi,\nu}(6)$, and $SU_{\pi,\nu}(3)$ symmetries. In these limits the g.s. band is fully symmetric. Since the states of the g.s. band in the $N < 82$ Ba isotopes have a quite strongly predominant $F_{\max}$ component (Figs. 13 and 14), and, as mentioned above, the states in the $N > 82$ Ba isotopes are fully symmetric, for the comparison one has only to consider the n_d distributions. Those concerning the three limits of the model are reported in Figs. 18 and 19.

In the $U_{\pi,\nu}(5)$ symmetry each state has just one n_d component (see Fig. 12), whichever is the boson number. In the $O_{\pi,\nu}(6)$ and $SU_{\pi,\nu}(3)$ symmetries the wave functions, which depend on the N_π and N_ν values, can be expanded in $U_{\pi,\nu}(5)$ basis states.

TABLE III. Experimental $B(M1)$ values (in μ_N^2 units) are compared to the calculated ones (in italics). The experimental $B(M1; 2_2^+ \rightarrow 2_1^+)$ transition strength of ^{126}Ba has been deduced from the $B(E2)$ and δ values of the transition.

$J_i \rightarrow J_f$	^{126}Ba	^{128}Ba	^{132}Ba	^{134}Ba
$2_2^+ \rightarrow 2_1^+$	$0.0021^{+0.0009}_{-0.0017}$	$0.0003(5)$	$0.0018(18)$	$0.0013(5)$
	0.0020	*0.0022*	*0.0029*	*0.0032*
$3_1^+ \rightarrow 2_1^+$				$0.00011(4)$
				0.00003
$3_1^+ \rightarrow 2_2^+$				$0.00003(2)$
				0.0033
$4_2^+ \rightarrow 4_1^+$		$0.00013(3)$		
		0.0090		

In the $O_{\pi,\nu}(6)$ symmetry each state can have multipole n_d components, whose values are all even or all odd. By looking at Fig. 18 and 19 it is seen how the difference between the n_d distribution of the g.s. band in the $U_{\pi,\nu}(5)$ and $O_{\pi,\nu}(6)$ symmetries increases as N_ν increases. This is particularly evident in the low-spin states, where the number of n_d components is larger than in the states of higher J. For example, in Fig. 18(b) [$N_\nu = 2$], the n_d components of the $J = 8$, 10 states are the same as those of the corresponding states in the $U_{\pi,\nu}(5)$ limit, while the 0^+ state has $n_d = 0$, $n_d = 2$ (predominant), and $n_d = 4$ components. In Fig. 18(e) [$N_\nu = 6$] the 0^+ state has a negligible $n_d = 0$ component, $n_d = 2$ and $n_d = 6$ components of comparable percentage, and the $n_d = 4$ as the strongest one. At the same time, the $n_d = 6$ has become predominant in the $J = 8$ state and $n_d = 7$ component has a large percentage in the $J = 10$ state.

In the $SU_{\pi,\nu}(3)$ limit each state has multiple n_d components, which span all the values between the minimum and the maximum. Strongly predominant n_d components are no longer present and the distribution becomes more and more flat as the boson number increases. This gives rise to a remarkable difference with the $O_{\pi,\nu}(6)$ symmetry, particularly evident when comparing Figs. 19(h) and 19(g) [$N_\nu = 8$].

Starting from the $N < 82$ Ba isotopes, it is now possible to compare the wave functions of the states belonging to the g.s. band with the corresponding ones in the three limits. As shown in Figs. 13 and 14, these states have a strongly predominant $F_{\max}$ component. The small percentage of the $F_{\max} - 1$ components reduces for increasing J, that of $F_{\max} - 2$ components keeps always negligible.

TABLE IV. Comparison of calculated (in italics) and experimental $B(E2)$ reduced transition probabilities (in e^2 b^2 units) in the even $^{122-134}$Ba isotopes.

$J_i \to J_f$	^{122}Ba	^{124}Ba	^{126}Ba	^{128}Ba	^{130}Ba	^{132}Ba	^{134}Ba
$2_1^+ \to 0_1^+$	0.475(26)[a]	0.415(18)	0.350(18)	0.276(27)	0.227(7)	0.172(12)	0.136(2)
	0.487	*0.395*	*0.337*	*0.284*	*0.229*	*0.188*	*0.143*
$4_1^+ \to 2_1^+$	0.600^{+120}_{-70}	0.626(15)[b]	0.480(10)	0.414(19)	0.309(5)		0.214(22)
	0.716	*0.575*	*0.491*	*0.417*	*0.337*		*0.195*
$4_1^+ \to 2_2^+$							0.0007(7)
							0.0024
$6_1^+ \to 4_1^+$	0.770(60)	0.637(24)[b]	0.649(28)	0.383(35)	0.368(23)		
	0.800	*0.634*	*0.532*	*0.446*	*0.353*		
$8_1^+ \to 6_1^+$	0.470(70)	0.643(74)[b]	0.812(58)[c]	0.364(50)	0.352(117)		
			0.162(18)[d]				
	0.835	*0.650*	*0.531*	*0.431*	*0.326*		
$10_1^+ \to 8_1^+$	⩾0.460		0.741(87)[c]	0.249(38)	0.211(27)		
			0.165(28)[d]				
	0.839		*0.519*	*0.404*	*0.299*		
$2_2^+ \to 0_1^+$				0.013(2)		0.015(6)	0.0015(5)
				0.012		*0.002*	*0.0002*
$2_2^+ \to 2_1^+$				0.123(15)		0.575(56)	0.239(22)
				0.123		*0.156*	*0.180*
$4_2^+ \to 2_1^+$				0.0035(3)			
				0.0035			
$4_2^+ \to 2_2^+$				0.238(23)			
				0.173			
$4_2^+ \to 4_1^+$				0.062(6)			
				0.044			
$6_2^+ \to 4_1^+$				0.0030(4)			
				0.0017			
$6_2^+ \to 4_2^+$				0.379(50)			
				0.244			
$8_2^+ \to 6_1^+$				0.0038(15)			
				0.0048			
$8_2^+ \to 6_2^+$				0.498(192)			
				0.196			
$10_2^+ \to 8_2^+$				0.383(115)			
				0.182			
$3_1^+ \to 2_1^+$							0.00010(3)
							0.00030
$3_1^+ \to 2_2^+$							0.018(3)
							0.162

[a]Weighted average of Refs. [49,57].
[b]Reference [58].
[c]Reference [59].
[d]Weighted average of data from Refs. [60–62].

By looking at Figs. 15 and 16, it is seen that in going from the heavier isotopes towards the neutron midshell there is a gradual change from an $U_{\pi,\nu}(5)$ to an $SU_{\pi,\nu}(3)$ structure. In ^{134}Ba [$N_\nu = 2$] the strongly predominant $n_d = 0, 1, 2$ components of the $J = 0, 2, 4$ states, respectively, are just those of the $U_{\pi,\nu}(5)$ symmetry.

In going towards ^{128}Ba the percentage of the $n_d = 3$ component in the 2^+ state and of the $n_d = 4$ component in the 4^+ state, characteristic of the $O_{\pi,\nu}(6)$ symmetry, increases, but the $U_{\pi,\nu}(5)$ structure keeps predominant. At the same time, indications of a slow raising of the $SU_{\pi,\nu}(3)$ contribution, as N reduces, stem from the presence of small n_d components, which, in the range of possible values, makes the distribution

continuous for all states, apart from the 0^+ state, where the $n_d = 1$ component is obviously missing.

In ^{126}Ba [$N_\nu = 6$] important $n_d = 0$ and $n_d = 1$, $U_{\pi,\nu}(5)$ components are present in the 0^+ and 2^+ states, respectively. The $U_{\pi,\nu}(5)$ components are predominant in the high spin states, as it turns out by comparing, for example, the relative percentage of the $n_d = 4, 6$ components in the 8^+ state with those in the $O_{\pi,\nu}(6)$ and $SU_{\pi,\nu}(3)$ n_d distributions [Figs. 18(e) and 18(f)]. Similar comments apply to ^{124}Ba.

In ^{122}Ba [$N_\nu = 8$], where the maximum deformation is attained, the n_d distribution is still far from that expected for an $SU_{\pi,\nu}(3)$ nucleus with the same number of bosons (Fig. 19). The $n_d = 0$ and $n_d = 1$ components of the 0^+ and 2^+ states,

TABLE V. Experimental $\delta(E2/M1)$ mixing ratios in the even $^{122-134}$Ba isotopes are compared to the absolute calculated values (in italics). Next to each predicted value the corresponding percentage of the $M1$ component is reported in bold face and square brackets (see text for details).

$J_i \to J_f$	^{122}Ba	^{124}Ba	^{126}Ba	^{128}Ba	^{130}Ba	^{132}Ba	^{134}Ba
$2_2^+ \to 2_1^+$		$M1$	$+5_{-1}^{+2}$	$+13_{-4}^{+16}$	$-0.30(1)$ or $-40(13)$ $-4.5(4)^a$	$+14_{-2}^{+3}$	$-7.4(9)$
		4.9 **[4]**	*3.9* **[6]**	*3.8* **[7]**	*2.6* **[13]**	*4.0* **[6]**	*3.5* **[8]**
$3_1^+ \to 2_1^+$		$M1$	$+5.5(10)$	$+4_{-1}^{+2}$	$-0.001(9)$ or $-4.6(2)$ $-4.5(4)^a$	$+2.2(1)$	$+0.8(1)$
		5.1 **[4]**	*5.0* **[4]**	*5.1* **[4]**	*2.9* **[11]**	*2.0* **[20]**	*8.3* **[1]**
$3_1^+ \to 2_2^+$			$E2(+M1)$	$[M1+E2]$	$+0.31(2)$ or $+13(3)$ $+20.(8)^a$	$+4.0(12)$	$+10(3)$
			4.6 **[5]**	*5.2* **[4]**	*4.3* **[5]**	*3.3* **[8]**	*2.8* **[11]**
$3_1^+ \to 4_1^+$		$M1$	$-1.7(2)$	$+4_{-1}^{+3}$	$-0.20(7)$ or $-2.5(5)$ $-21(10)^a$	$+6(1)$	$(M1+E2)$
		2.6 **[13]**	*2.4* **[15]**	*2.7* **[12]**	*1.4* **[34]**	*1.0* **[50]**	*0.7* **[67]**
$4_2^+ \to 3_1^+$							$[M1+E2]$
							-1.4 **[34]**
$4_2^+ \to 4_1^+$		$-0.15_{-0.20}^{+0.25}$	$+1.4_{-0.3}^{+8.0}$	-14_{-16}^{+8}	$-0.43(8)$ or $2.4(5)$	$-2.6(2)$	$+0.26(1)$
		1.7 **[26]**	*1.2* **[41]**	*1.1* **[45]**	*0.9* **[55]**	*1.3* **[37]**	*1.6* **[28]**
$5_1^+ \to 4_1^+$	$+3.7_{-1.0}^{+2.2}$ or $+0.30(12)$	$M1, E2$		$M1$			
	2.4 **[15]**	*2.9* **[11]**		*3.0* **[10]**			
$5_1^+ \to 6_1^+$		$M1$					
		1.5 **[31]**					
$6_2^+ \to 6_1^+$		$M1+E2$	$+2.8_{-0.9}^{+2.4}$				
		0.9 **[55]**	*0.6* **[74]**				
$7_1^+ \to 6_1^+$	$+0.6(4)$	$M1$					
	1.2 **[41]**	*1.8* **[24]**					
$8_2^+ \to 8_1^+$		$M1$					
		0.8 **[61]**					

^{a}Reference [6].

respectively, are close to 20%. The predominant components of the $J = 6, 8, 10$ states are still those of the $U_{\pi,\nu}(5)$ limit, as it turns out from the comparison with those having the same spin in the three limits of the model, for $N = 8$ (Figs. 18 and 19). The n_d distribution in ^{120}Ba [$N_\nu = 7$] is quite similar to that of ^{122}Ba, but, as revealed by Fig. 2, its deformation is larger.

In ^{118}Ba [$N_\nu = 6$], where the transition from the maximum deformation towards the $U_{\pi,\nu}(5)$ symmetry is beginning, the deformation is larger than in ^{126}Ba, which has the same N_ν. This is related to the fact that the particle-proton, particle-neutron bosons interaction in the $N < 66$ region is larger than the particle-proton, hole-neutron bosons interaction in the $N > 66$ region (see, e.g., Refs. [65,66]).

TABLE VI. Experimental excitation energies (in keV) of the 0_2^+ states in the even $^{124-132}$Ba isotopes are compared to the calculated ones (in italics).

	^{124}Ba	^{126}Ba	^{128}Ba	^{130}Ba	^{132}Ba
E_{lev}	1071	983	942	1180	1503
	1091	*1014*	*1006*	*1054*	*1308*

Moving now to the $N > 82$ region, it is possible to compare the structure of the g.s. band of an isotope belonging to the [50–82] neutron shell with that of the corresponding isotope (same N_ν) in the [82–126] neutron shell. It turns out that the couples of isotopes of same N_ν, from (^{134}Ba, ^{142}Ba; $N_\nu = 2$) to (^{128}Ba, ^{148}Ba; $N_\nu = 5$), have rather similar n_d structures, even though a larger spread of the n_d components reveals a higher deformation in the neutron-rich isotopes.

A sudden onset of deformation appears in ^{150}Ba ($N = 94$), as shown by the increased number of n_d components in each state and by their close percentages. This is at variance with what observed in ^{118,126}Ba, which have the same N_ν, and in the neighboring ^{148}Ba isotope. By comparing the n_d components of ^{150}Ba with those of ^{122}Ba the difference in deformation is striking.

An abrupt increase of deformation in the $A = 150$ region is a well-known phenomenon observed in even $Z > 56$ isotopic chains. It is related to the fact [67] that when neutrons, near to $N = 90$, start filling the $\nu h_{9/2}$ orbit the strong interaction with the protons occupying the $\pi h_{11/2}$ spin-orbit partner leads to a significant lowering of the particle energies of both these orbits with respect to their neighbors. The lowering of the $\pi h_{11/2}$ orbit gives rise to the obliteration of the gap at $Z = 64$ (midshell at $N = 57$) and to an increase of the effective valence proton number of Ce ($Z = 58$) and Nd ($Z = 60$) nuclei
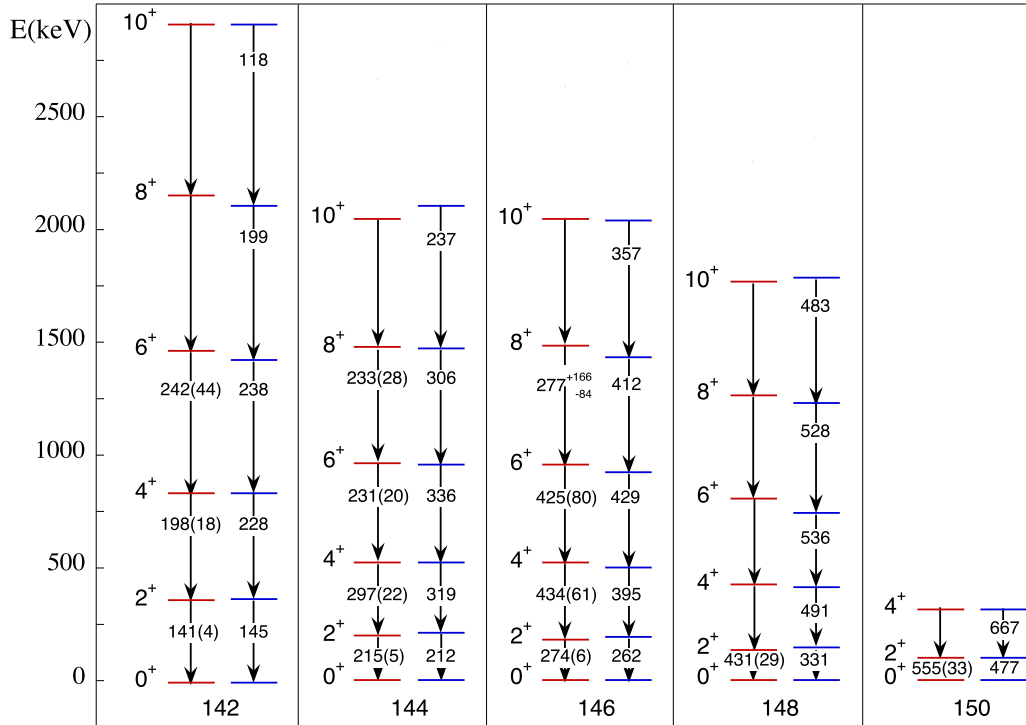
FIG. 11. Comparison of experimental (left) and calculated (right) excitation energies and $B(E2)$ transition strengths (in $10^{-3}e^2$ b^2 units) in $^{142-150}$Ba isotopes. The $B(E2)$ transition strengths of the $2_1^+ \rightarrow 0_1^+$, $4_1^+ \rightarrow 2_1^+$, $6_1^+ \rightarrow 4_1^+$, and $8_1^+ \rightarrow 6_1^+$ values in ^{144}Ba are the weighted averages of the data extracted from Refs. [51–53] for the first three transitions and from Refs. [52,53] for the last one. In ^{146}Ba the $B(E2; 4_1^+ \rightarrow 2_1^+)$ value is the weighted average of the data extracted from Refs. [54,55], the $B(E2; 6_1^+ \rightarrow 4_1^+)$ and $B(E2; 8_1^+ \rightarrow 6_1^+)$ have been deduced from Ref. [55]. The excitation energies of ^{150}Ba and the $B(E2; 2_1^+ \rightarrow 0_1^+)$ transition strengths of ^{148,150}Ba are from Ref. [56].
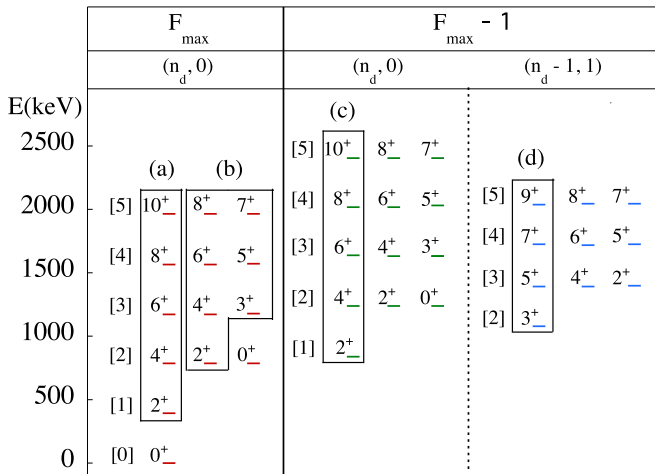

FIG. 12. Eigenstates of the $U_{\pi,\nu}(5)$ Hamiltonian $H = \varepsilon\,(\hat{n}_{d_\pi} + \hat{n}_{d_\nu}) + \hat{M}_{\pi\nu}$, of a nucleus having $N_\pi = 3$ and $N_\nu = 4$. Only the states of spin $J \leqslant 10$ are shown. Fully symmetric states are displayed together with $F = F_{\text{max}} - 1$ states whose energy does not depend on the parameter ξ_1. At the top of each group are shown the quantum number (n_1, n_2) of the relevant $U_{\pi,\nu}(5)$ representation. On the left of each degenerate multiplet the number of d boson is reported in square brackets. Only the three states of highest spin for each multiplet are show. The subsets of states enclosed in frames (a), (c), and (d) are of particular interest for the discussion (see text).

(stronger in the latter one), while that of nuclei with $Z < 57$ does not change. Such an effect is clearly visible in Fig. 1. The $R_{4/2}$ ratio of the Ba, Ce, and Nd isotones has the largest value for Ba and the smaller one for Nd up to $N = 88$, at $N = 90$ the situation reverses.

The strong deformation increase observed in going from ^{148}Ba to ^{150}Ba ($N = 94$) should instead be ascribed to the lowering of the $\nu h_{9/2}$ orbit. In fact, the presence of a bump at $N = 90$ (Fig. 5), indicates a partial subshell closure of the $\nu f_{7/2}$ orbital (midshell $N = 86$) originated by the gap it forms with the $\nu h_{9/2}$ orbits. It gradually disappears when the neutrons start filling the latter orbit, giving rise to an increase of the effective valence neutron number. The presence of such a gap explains why the excitation energies of ^{144}Ba and ^{146}Ba ($N = 90$) are so close.

The conclusions one can draw from the analysis of the wave functions of the g.s. band all along the isotopic chain is that both the neutron-deficient and neutron-rich Ba isotopes perform an $U_{\pi,\nu}(5) \rightarrow \text{SU}_{\pi,\nu}(3)$ transition in moving away from the $N = 82$ closure shell.

For the $N < 82$ isotopes the present findings are in line with the interpretation proposed in the late 1990's by Zamfir *et al.* [31], according to which the apparent $O_{\pi,\nu}(6)$ symmetry character displayed by the $N \simeq 72$–76 Ba isotopes would correspond to a region of a $U_{\pi,\nu}(5) \rightarrow \text{SU}_{\pi,\nu}(3)$ transition. In the $N > 82$ isotopes the possibility of correctly matching the trend of the excitation energies and the $E2$ reduced transition
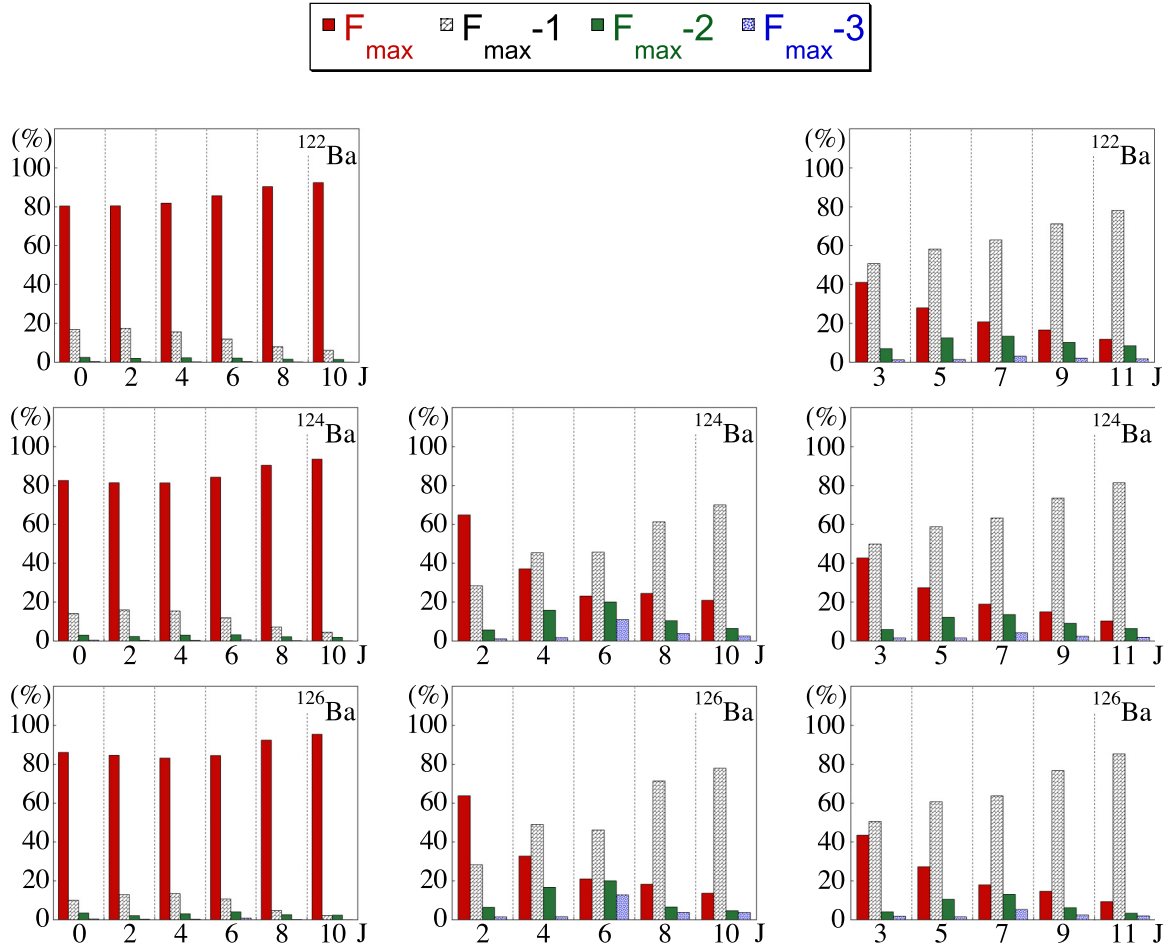
FIG. 13. F-spin components (amplitude square) of the states of the g.s. band (left group) and of the even-spin (central group) and odd-spin (right group) states of the γ bands in even $^{122-126}$Ba isotopes.

strengths of the g.s. band points out the quadrupole collectivity of this band.

Finally, the present study makes it possible to know the approximate structure of a nucleus near the X(5) critical point of the $U_{\pi,\nu}(5) \rightarrow$ SU$_{\pi,\nu}(3)$ shape phase transition. Indeed, as shown in Fig. 2, the curve representing the X(5) curve in the $N < 82$ isotopes is between those of ^{118}Ba and ^{122}Ba and that in the $N > 82$ isotopes between those of the ^{146}Ba and ^{148}Ba. The n_d distribution, which is rather similar in these isotopes, shows how the $U_{\pi,\nu}(5)$ structure is still predominant when the X(5) critical point is reached.

B. γ band structure in the $N < 82$ Ba isotopes

Before discussing the γ band structure in the $N < 82$ Ba isotopes it is worth mentioning that also in the O$_{\pi,\nu}(6)$ symmetry there are two $F = F_{\max} - 1$ groups of states with characteristics analogous to those of the groups of states reported in column (c) and (d) of Fig. 12 for the $U_{\pi,\nu}(5)$ symmetry.

In the $N < 82$ Ba isotopes, the difference in the proton-neutron symmetry between the g.s. band and the γ band clearly shows up when looking at Figs. 13 and 14. Apart from

the 2_2^+ state, all the members of the γ band have predominant MS character. The amplitude square of the $F_{\max}$ component decreases, as a function of J, in both the even- and odd-spin branches and in most cases, for the states of highest spin, drops to a percentage of $\simeq 10\%$. Among the $F < F_{\max}$ components, the $F_{\max} - 1$ component is the strongly predominant one, reaching in many cases percentages as high as $\simeq 80\%$. Obviously, these states do not correspond to states of the IBA-1 model.

Considering first the even-spin branch of the γ band, one can observe that the 2^+ state has large $F_{\max}$, $n_d = 2$ and important $F_{\max} - 1$, $n_d = 1$ components. By looking at Fig. 12, its structure should be mainly due to a mixing of the two 2^+ basis states belonging to columns (a) and (c). As to the states with spin $J \geqslant 4$, it turns out from Figs. 15 and 16 that their structure evolution, in terms of n_d distributions, reflects very closely that of the states with the same spin of the g.s. band. In $^{126-130}$Ba the n_d components of the corresponding states in the two bands have a percentage difference within a few percent. Taking also into account the predominant MS component of these states, the similarity of their structure with that of the states of column (c) in Fig. 12 is evident, particularly for the heavier isotopes and for the states of highest spin in the
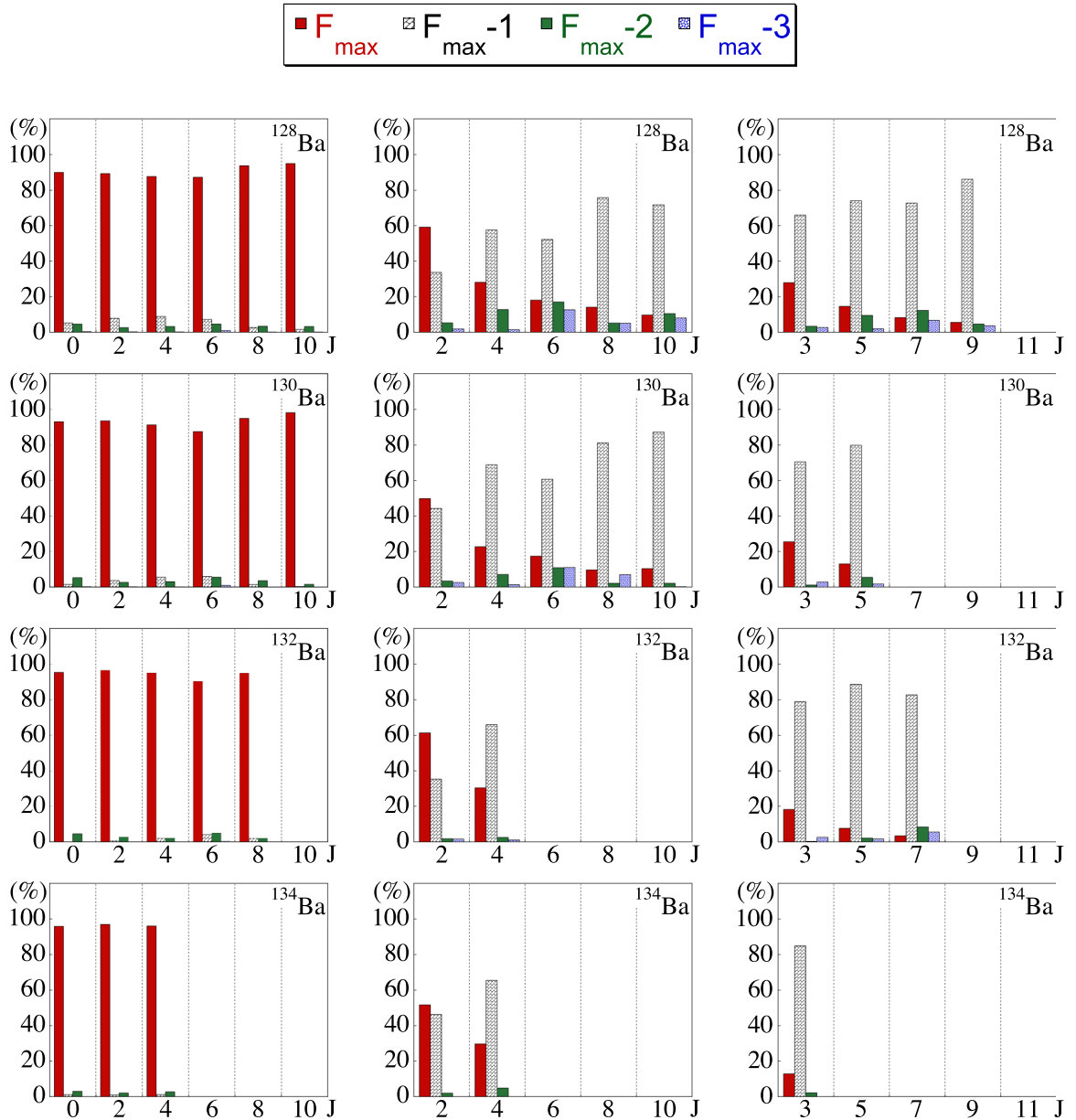
FIG. 14. As Fig. 13, for even $^{128-134}$Ba isotopes.

lighter ones. This reflects what is observed in Sec. III A, i.e., that the $U_{\pi,\nu}(5)$ structure keeps a predominant role in the evolution of the isotopic chain towards its maximum deformation. As to the odd-spin states, in $^{130-134}$Ba, in spite of the limited number of known collective states, it is evident that the structure of the states corresponds to that of the states of column (d) in Fig. 12. In ^{128}Ba, where a well-developed band is known, the $J = 5, 7, 9, 11$ states have just one n_d component strongly predominant, that is, $n_d = 4, 5, 6, 7$ component, respectively. Such components maintain still predominant in the lighter isotopes, even though with a reduced percentage. It is worth mentioning that in a realistic IBA-1 γ band, having a structure close to that reported in column (b) of Fig. 12, the $J = 5, 7, 9, 11$ states would have predominant $n_d = 4, 5, 6, 7$ components, respectively.

An interesting and very particular feature of the γ band is the odd-even spin energy staggering displayed by its levels. Such an effect has been observed in different mass regions and extensively investigated because of the important clues it can provides about the nuclear structure. Models to distinguish between quadrupole deformed nuclear shapes with soft triaxiality [68,69] and with rigid triaxiality [70] have been proposed since the 1950's. The problem of the triaxiality extent in nuclei and of a possible stable triaxial deformation in the nuclear ground states is still a matter of debate.

In the framework of the IBA-1 model, where the shape of the nucleus can only be prolate, oblate or γ unstable, the explanation of the staggering effect in some barium and xenon isotopes was obtained by Casten *et al.* [71] by adding to the usual Hamiltonian a three-body term leading to a triaxial de-
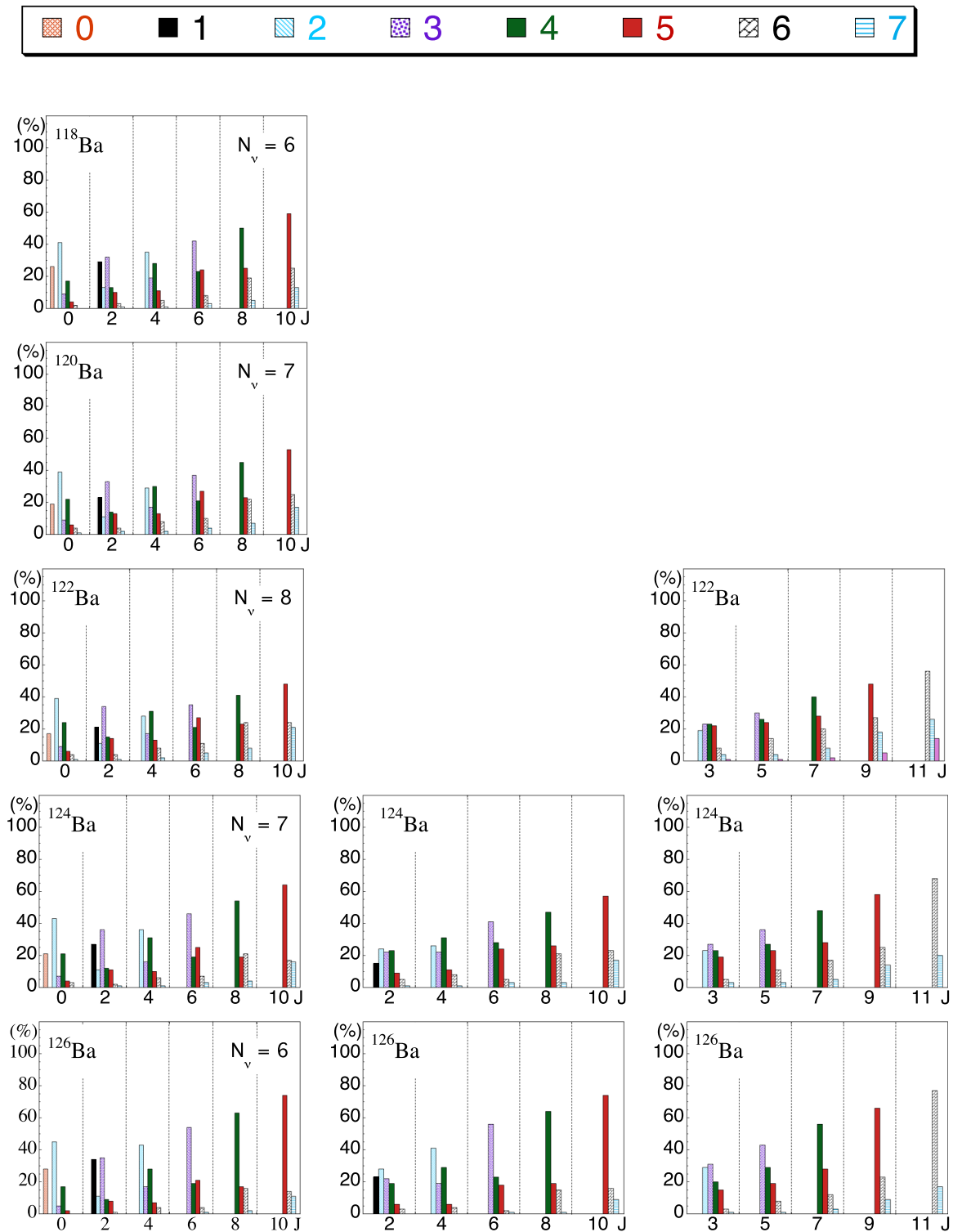
FIG. 15. n_d components (amplitude square) of the states of the g.s. band (left column) and of the even-spin (central column) and odd-spin (right column) states of the γ band in even $^{122-126}$Ba isotope. The symbols utilized for the different n_d values are shown at the top of the figure. The $n_d = 8$ component, normally negligible, is not reported.

formation. The importance of the inclusion of the three-body term has been studied also recently by Sorgunlu and Van Isacker [72] in a study of isotopes close to the O(6) symmetry including even $^{128-132}$Ba isotopes.

As to the present work, the comparison of the experimental and predicted spin staggering, in the isotopes where both even and odd branches of the γ band are sufficiently developed, has been made utilizing the
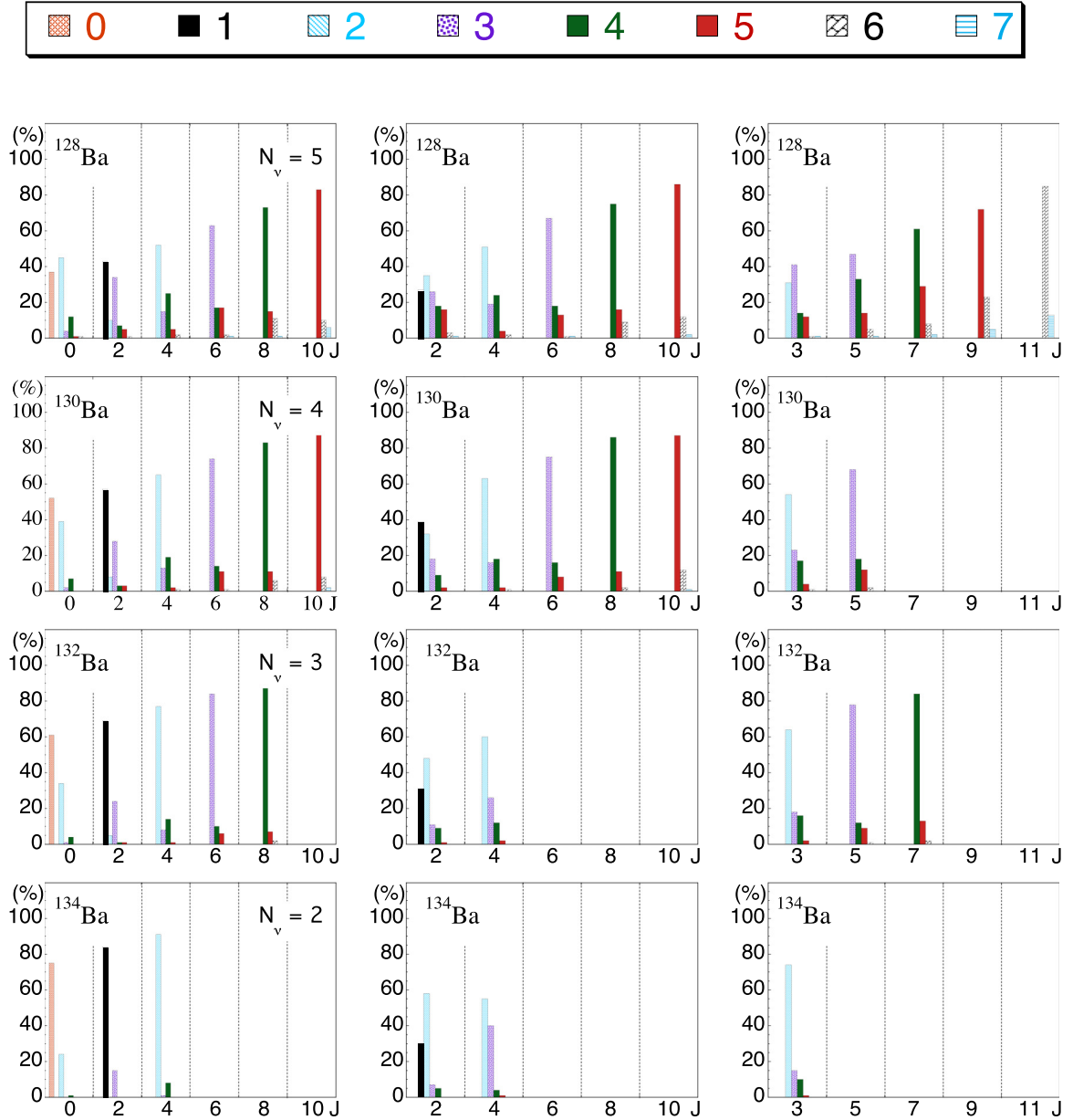
FIG. 16. As Fig. 15, for even $^{128-134}$Ba isotope.

expression [73]

$$S(J) = \frac{E(J)E(J-1)}{E(J) - E(J-2)}$$
$$\frac{(J(J+1) - (J-1)(J-2)}{J(J+1) - J(J-1)} - 1, \quad (6)$$

which vanishes in absence of an even-odd staggering.

The results are displayed in Fig. 20. Noticeably, the rather good agreement obtained strongly depends on the choice of the Majorana parameters ξ_2 and ξ_3 (see Fig. 4 for the latter).

To summarize, in the present interpretation the γ band, is made up of two branches, corresponding to a large extent to the $F = F_{\max} - 1$ groups of states reported in Fig. 12 which have $(n_d, 0)$ (even-spin states) and $(n_d - 1, 1)$ (odd-spin states) quantum numbers. The properties of these states

are smoothly changing as a function of the neutron number, as required for states of collective nature.

C. Decay of the γ bands in the $N < 82$ Ba isotopes

Having investigated the structure of the relevant states, it is now possible to point out some specific properties of the γ band decay. In the cases of interest for the present work it is possible to identify three different ways of decay. They are first schematically discussed in the $U_{\pi,\nu}(5)$ symmetry, where the $\langle \|\hat{T}_\pi(E2)\| \rangle$ and $\langle \|\hat{T}_\nu(E2)\| \rangle$ matrix elements of a transition connecting two $\Delta F = \pm 1$ states have the same absolute value but opposite sign [74].

(i) $\Delta F = 0$, $\Delta n_d = 1$. This is the case of the in-band transitions of the two branches of the γ band.
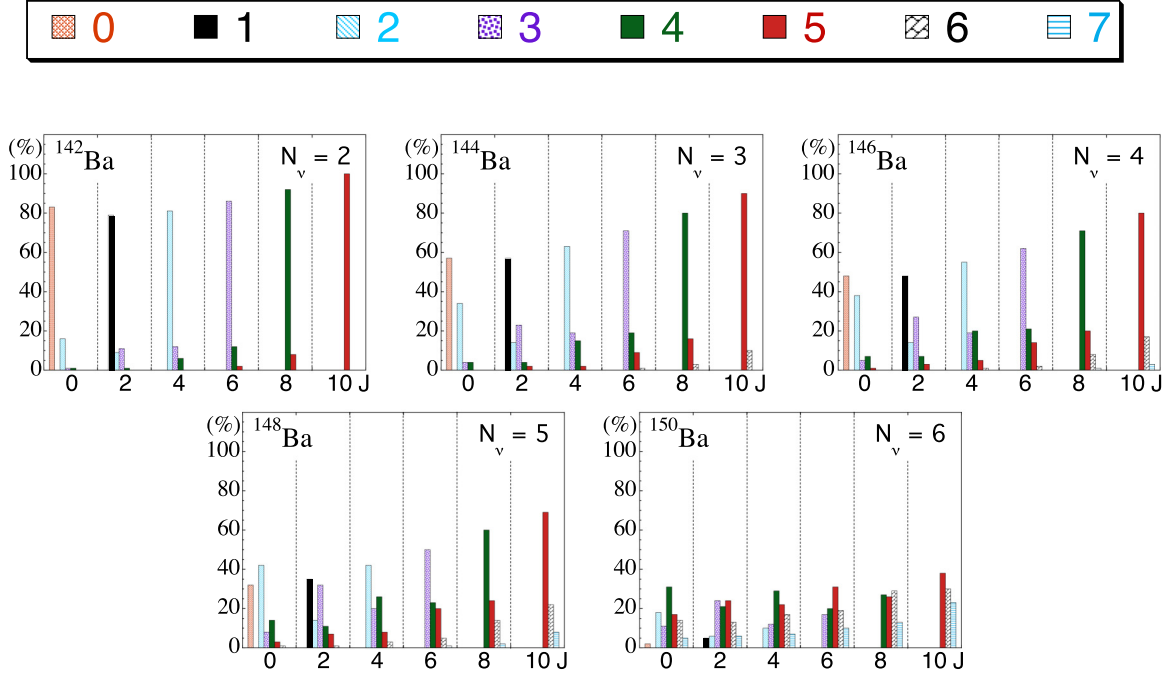
FIG. 17. As Fig. 15, for even $^{142-150}$Ba isotope.

(ii) $\Delta F = -1$, $\Delta n_d = 0$. Because of the expression of Eq. (2) the transition probability is proportional to $(e_\nu \chi_\nu - e_\pi \chi_\pi)^2$. Such a kind of transition can connect
    (a) a state of the γ band of even-spin J to the state of the g.s. band with the same spin (ex., $4_\gamma^+ \to 4_1^+$);
    (b) a state γ band of odd-spin J to the state of the g.s. band of spin $(J+1)$ (ex., $5_\gamma^+ \to 6_1^+$).

(iii) $\Delta F = -1$, $\Delta n_d = 1$. Because of the expression of Eq. (2) the transition probability is proportional to $(e_\nu - e_\pi)^2$. Such a kind of transition can connect
    (a) a state of the γ band of even-spin J to the $(J-2)$ state of the g.s. band (e.g., $4_\gamma^+ \to 2_1^+$);
    (b) a state of the γ band of odd-spin J to the $(J-1)$ state of the g.s. band (e.g., $3_\gamma^+ \to 2_1^+$).

Coming now to the Ba isotopes, the three different modes of decay just described are recognizable in the transitions connecting the states of the even-spin and odd-spin branches of the γ band to those of the g.s band. In transitions corresponding to case (i) the $\langle \|\hat{T}_\nu(E2)\| \rangle$ and $\langle \|\hat{T}_\pi(E2)\| \rangle$ matrix elements normally have rather large values and equal sign, so that the calculated $B(E2)$ values,

$$B(E2) = \frac{(e_\nu \langle \|\hat{T}_\nu(E2)\| \rangle + e_\pi \langle \|\hat{T}_\pi(E2)\| \rangle)^2}{2(J+1)} \quad (7)$$

are large and of the same order of magnitude as those in the g.s. band. Their values are only slightly affected by changes of the effective charges in a reasonable range of values.

In transitions corresponding to cases (ii) the proton and neutron contributions to the transition probability add, because χ_π and χ_ν have opposite sign in all the isotopes, apart

from ^{122}Ba (see Table I). Normally, the absolute value of the $E2$ matrix elements are smaller than those of case (i).

In transitions corresponding to case (iii) it turns out that the $\langle \|\hat{T}_\pi(E2)\| \rangle$ and $\langle \|\hat{T}_\nu(E2)\| \rangle$ matrix elements have opposite sign and absolute values that tend to approach in going towards high spin states where the $F_{max} - 1$ percentage is rather high. As a consequence, cancellation effects originated by the close values of the effective charges can drastically affect the $B(E2)$ values, and small variations of e_ν and e_π can induce dramatic changes. The outlined transition modes help understanding why the predicted $E2$ transitions can span three orders of magnitude, as the experimental data do.

Examples corresponding to the decay modes just described can be found in ^{128}Ba, which is the isotope where the richest information on $E2$ transitions is available (see Table IV).

(i) The $B(E2)$ values of the in-band transitions of each branch of the γ band are in the same range $(0.200/0.500 \ e^2 \ \text{b}^2)$ as those of the g.s. band.

(ii) The $B(E2; 4_2^+ \to 4_1^+)$ transition strength has a value $(0.062 \ e^2 \ \text{b}^2)$ definitely lower than those of case (i).

(iii) The $B(E2)$ values of the $4_2^+ \to 2_1^+$, $6_2^+ \to 4_1^+$, $8_2^+ \to 6_1^+$ transitions $(\simeq 0.0035 e^2 \ \text{b}^2)$ are about two orders of magnitude lower than those of case (i).

As to the $M1$ transitions, since their probabilities are proportional to $(g_\pi - g_\nu)^2$, to have separate information on the gyromagnetic ratios, one has to consider the magnetic moments, in the expression of which g_ν and g_π take independent values. The agreement between calculated and experimental magnetic moments (see Table II) indicates that both coefficients have been correctly fixed.
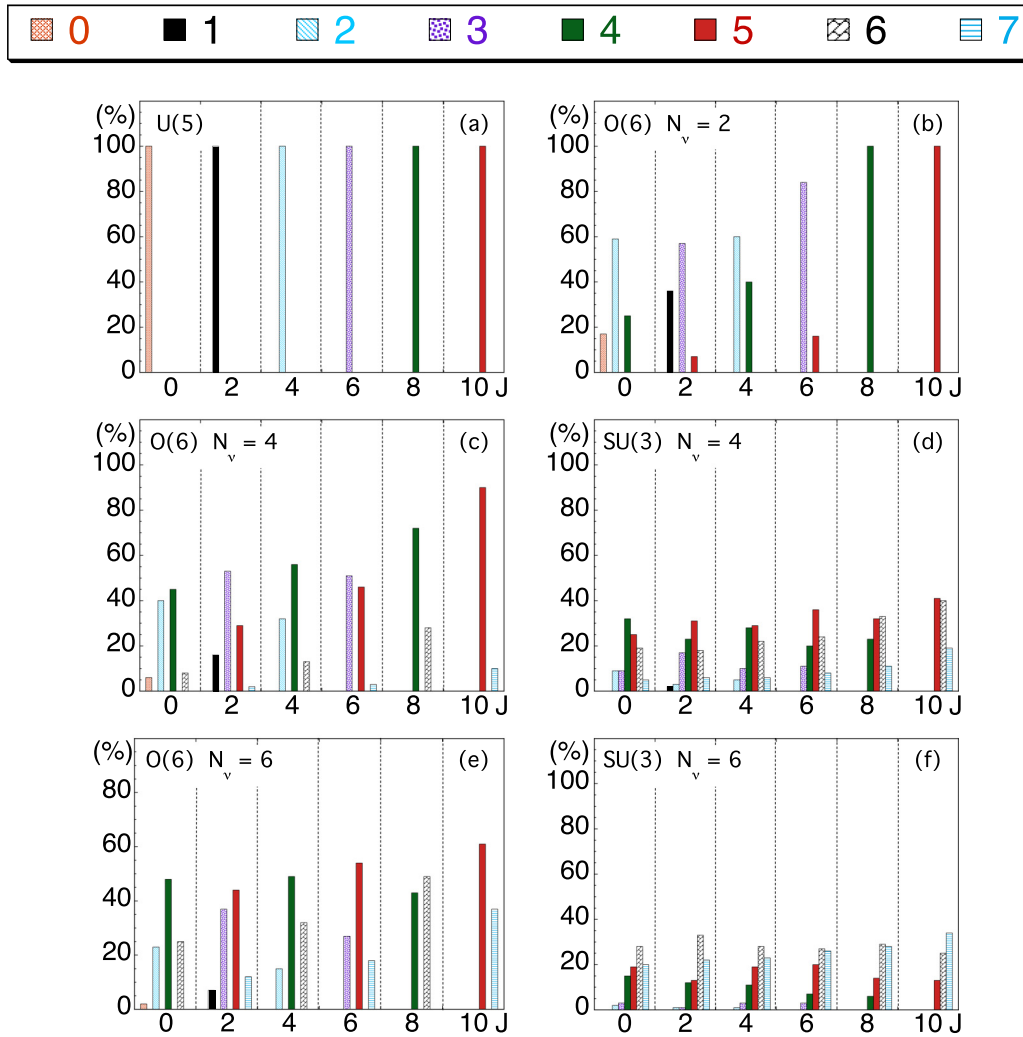
FIG. 18. n_d components (amplitude square) of the states of the g.s. band in the $U_{\pi,\nu}(5)$, $O_{\pi,\nu}(6)$, and $SU_{\pi,\nu}(3)$ symmetries. In the $O_{\pi,\nu}(6)$ and $SU_{\pi,\nu}(3)$ limits, they have been evaluated for $N_\pi = 3$ and for the N_ν values reported in each panel. The symbols utilized for the different n_d values are shown at the top of the figure. The $n_d = 8$ component, normally negligible, is not reported.
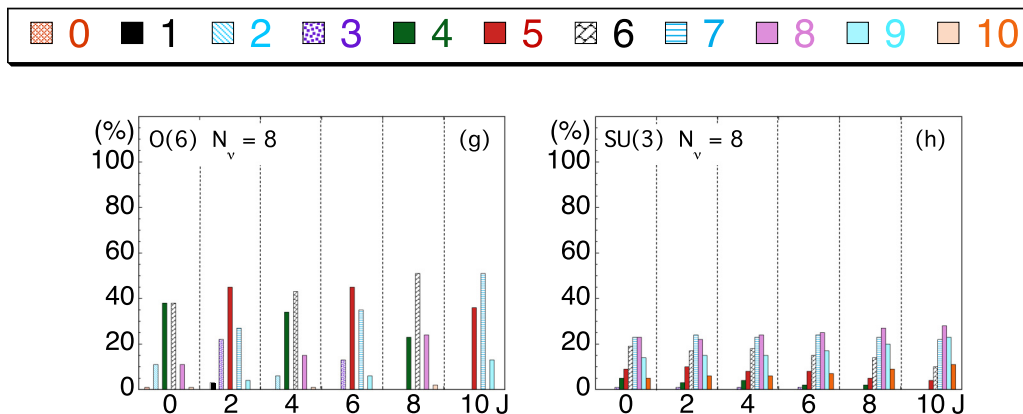

FIG. 19. n_d distributions in the $O_{\pi,\nu}(6)$ and $SU_{\pi,\nu}(3)$ models for $N_\pi = 3$ and $N_\nu = 8$. The symbols utilized for the different n_d values are shown at the top of the figure.
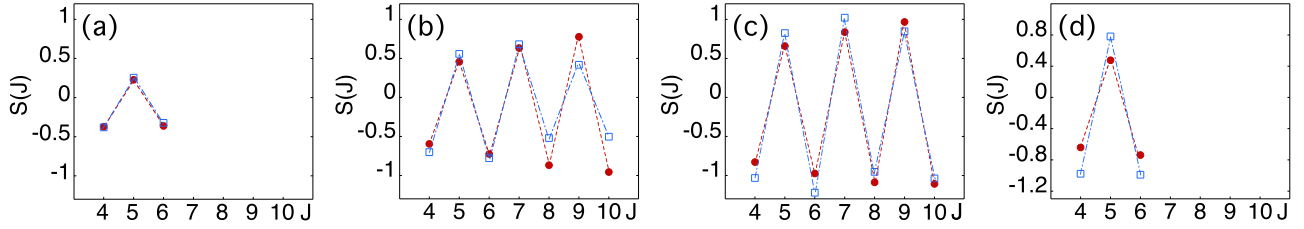
FIG. 20. Observed (circles) and calculated (squares) signature splitting, S, of the γ bands in (a) ^{124}Ba, (b) ^{126}Ba, (c) ^{128}Ba, and (d) ^{130}Ba.

As shown in Table III, the information on $B(M1)$ transition strengths is extremely limited and in four cases out of seven it concerns the $2_2^+ \to 2_1^+$ transitions (in ^{126,128,132,134}Ba). Because the 2_1^+ states have FS character, the 2_2^+ states have a large FS component, and the n_d distribution is not very similar in the initial and final states, particularly in the heavier isotopes, the $M1$ transitions are partially forbidden. Their order of magnitude is $10^{-3}\mu_\nu^2$.

Additional information on $M1$ transitions can be obtained from the analysis of branching ratios and mixing ratios. As it turns out from Table V, it can happen that in a transition connecting a state of the γ band, which has predominant MS components, to one of the g.s. band, of FS character, the $M1$ component competes with the $E2$ component. It is important to distinguish if this is due to a small $E2$ component or to a strong $M1$ component.

In the realistic case of Ba isotopes, where multiple F-spin and n_d components are present in the relevant wave functions, one can just give some schematic explanation of how the two cases happen. The first one concerns $\Delta F = -1$, $\Delta n_d = 1$ transitions. This means $E2$ transitions of type (iii), which are very weak because of the cancellation effects, and $M1$ transitions, which are mainly forbidden, because of the selection rule $\Delta n_d = 0$, but have strengths larger than those of the competing $E2$ transitions. As an example, it is possible to consider the $7_1^+ \to 6_1^+$ transition in ^{122}Ba. Both the predicted $E2$ and $M1$ reduced transition strengths are small [$B(E2) = 0.0037e^2$ b^2, $B(M1) = 0.0020\mu_N^2$], but the $M1$ percentage is 41% (Table V). The experimental branching ratio of 7_1^+ level and the mixing ratio of the $7_1^+ \to 6_1^+$ transition are reasonably reproduced. In the second case, $\Delta F = -1$, $\Delta n_d = 0$, the $E2$ transitions are of type (ii), so do not have strong $B(E2)$ values, whereas the $M1$ transitions are allowed.

It is possible to take as examples the transitions connecting the $J \geqslant 4$ even-spin states of the γ band with the states of same J of the g.s. band. In the $4_2^+ \to 4_1^+$ transitions in $^{124-132}$Ba the predicted $M1$ percentages (Table V) are always large; in ^{130}Ba the $M1$ component is predominant. As shown in Figs. 7–9, in the observed decay of the 4_2^+ states, the $4_2^+ \to 4_1^+$ transition is the strongest one in ^{124,126,130}Ba and has a large percentage in ^{128,132}Ba. The possibility of reproducing the branching ratios of the 4_2^+ states and the order of magnitude of δ in the $4_2^+ \to 4_1^+$ transitions is strongly due to the presence of the $M1$ components. For the transitions of this type deexciting the states of higher spin the calculations predict an increase of the $B(M1)$ values, because the wave functions of the initial and final states match better the conditions concerning F spins and n_d distributions that allow

$M1$ transitions. No significant change is instead predicted for the competing $B(E2)$ transition strength. This reflects on the calculated $M1$ percentages in the $6_2^+ \to 6_1^+$, and $8_2^+ \to 8_1^+$ transitions (Table V), therefore in a reduction of the δ values. When the comparison is possible, it is seen that the calculations are able to correctly reproduce the branching ratios of the initial level as well as the mixing ratio of the transitions. In the cases just discussed of allowed $M1$ transitions the order of magnitude of the calculated $B(M1)$ transition strength turns out to be $\simeq 10^{-2}\mu_N^2$.

IV. CONCLUSIONS

The collective states of the g.s. band in the $^{118-134,142-150}$Ba and of the γ band in $^{122-134}$Ba isotopes have been studied in the framework of the IBA-2 model, taking into account excitation energies and all available e.m. properties. Only three parameters have been adjusted in the analysis of the g.s. band and five in that of the γ band. The general satisfactory agreement between theory and experiment has stimulated the in-depth study of the wave function of the relevant states.

By comparing the structure of the Ba isotopes of interest with that of the three limits of the IBA-2 model it has been possible to study in detail the structure evolution of the isotopic chain over the [50–82] and [82–126] major shells reaching the conclusion that both the neutron-deficient and neutron-rich Ba isotopes perform an $U_{\pi,\nu}(5) \to$ SU$_{\pi,\nu}(3)$ transition in moving away from the $N = 82$ closure shell. In the $N < 82$ isotopes no isotope displays an outstanding O$_{\pi,\nu}(6)$ structure, even though n_d component characteristic of this symmetry contribute to the structure evolution. The different deformation in the $N < 82$ and $N > 82$ regions is to be ascribed, in part, to the different nature (hole or particle) that the neutron boson have in the different N regions, but, overall, to the underlying nuclear structure, with residual interactions between protons and neutrons in specific orbits.

In the $N < 82$ isotopes it has been pointed out the coexistence of a g.s. band of FS character and of a γ band of MS character, whose even-spin and odd-spin branches correspond, to a large extent, to two $U_{\pi,\nu}(5)$ group of states characterized by different quantum numbers. The relative excitation energies of the predicted even-spin and odd-spin branches of the γ band matches correctly the observed energy staggering in $^{124-130}$Ba isotopes. The specific decay modes of the two branches of the band have been discussed in detail. The cases where the presence of $M1$ transitions connecting the γ band to the g.s. band can be essential to reproduce the experimental data have been pointed out.

[1] F. Iachello and A. Arima, *The Interacting Boson Model* (Cambridge University Press, Cambridge, 1987).

[2] A. Arima, T. Otsuka, F. Iachello, and I. Talmi, Phys. Lett. B **66**, 205 (1977).

[3] T. Otsuka, A. Arima, and F. Iachello, Nucl. Phys. A **309**, 1 (1978).

[4] F. Iachello, Phys. Rev. Lett. **53**, 1427 (1984).

[5] A. Giannatiempo, P. Sona, and A. Nannini, Phys. Rev. C **62**, 044302 (2000).

[6] C. T. Königshofen, K. Jessen, A. Gade, I. Wiedenhöver, H. Meise, and P. von Brentano, Phys. Rev. C **64**, 037302 (2001).

[7] N. Pietralla, P. von Brentano, and A. F. Lisetskiy, Prog. Part. Nucl. Phys. **60**, 225 (2008).

[8] A. Hennig, T. Ahn, V. Anagnostatou, A. Blazhev, N. Cooper, V. Derya, M. Elvers, J. Endres, P. Goddard, A. Heinz, R. O. Hughes, G. Ilie, M. N. Mineva, P. Petkov, S. G. Pickstone, N. Pietralla, D. Radeck, T. J. Ross, D. Savran, M. Spieker, V. Werner, and A. Zilges, Phys. Rev. C **92**, 064317 (2015).

[9] A. M. A. Hussain, F. H. Al-khudair, and A. R. H. Subber, Turk. J. Phys. **39**, 137 (2015).

[10] T. Thomas, V. Werner, J. Jolie, K. Nomura, T. Ahn, N. Cooper, H. Duckwitz, A. Fitzler, C. Fransen, A. Gade, M. Hinton, G. Ilie, K. Jessen, A. Linnemann, P. Petkov, N. Pietralla, and D. Radeck, Nucl. Phys. A **947**, 203 (2016).

[11] T. Beck, J. Beller, N. Pietralla, M. Bhike, J. Birkhan, V. Derya, U. Gayer, A. Hennig, J. Isaak, B. Löher, V. Yu. Ponomarev, A. Richter, C. Romig, D. Savran, M. Scheck, W. Tornow, V. Werner, A. Zilges, and M. Zweidinger, Phys. Rev. Lett. **118**, 212502 (2017).

[12] A. Giannatiempo, Phys. Rev. C **96**, 044326 (2017).

[13] R. Stegmann, C. Stahl, G. Rainovski, N. Pietralla, C. Stoyanov, M. P. Carpenter, R. V. F. Janssens, M. Lettmann, T. Möller, O. Möller, V. Werner, and S. Zhu, Phys. Lett. B **770**, 77 (2017).

[14] R. Kern, R. Stegmann, N. Pietralla, G. Rainovski, M. P. Carpenter, R. V. F. Janssens, M. Lettmann, O. Moller, T. Möller, C. Stahl, V. Werner, and S. Zhu, Phys. Rev. C **99**, 011303(R) (2019).

[15] F. Iachello, Phys. Rev. Lett. **87**, 052502 (2001).

[16] A. Arima and F. Iachello, Ann. Phys. (NY) **123**, 468 (1979).

[17] G. Puddu, O. Scholten, and T. Otsuka, Nucl. Phys. A **348**, 109 (1980).

[18] R. F. Casten and P. von Brentano, Phys. Lett. B **152**, 22 (1985).

[19] A. Novoselsky and I. Talmi, Phys. Lett. B **172**, 139 (1986).

[20] H. Harter, P. O. Lipas, R. Nojarov, Th. Taigel, and A. Faessler, Phys. Lett. B **205**, 174 (1988).

[21] B. Fazekas, T. Belgya, G. Molnar, Á. Veres, R. A. Gatenby, S. W. Yates, and T. Otsuka, Nucl. Phys. A **548**, 249 (1992).

[22] T. Otsuka, Nucl. Phys. A **557**, 531c (1993).

[23] T. Otsuka, T. Mizusaki, and K. H. Kim, in *Perspectives for the Interacting Boson Model* (World Scientific, Singapore, 1994), p. 33.

[24] T. Mizusaki and T. Otsuka, Prog. Theor. Phys. Suppl. **125**, 97 (1996).

[25] M. Sugita, K. Uchiyama, and K. Furuno, Phys. Lett. B **440**, 239 (1998).

[26] A. Gade, I. Wiedenhöver, H. Meise, A. Gelberg, and P. von Brentano, Nucl. Phys. A **697**, 75 (2002).

[27] G. Suliman, D. Bucurescu, R. Hertenberger, H.-F. Wirth, T. Faestermann, R. Krücken, T. Behrens, V. Bildstein, K.

[28] Eppinger, C. Hinke, M. Mahgoub, P. Meierbeck, M. Reithner, S. Schwertel, and N. Chauvin, Eur. Phys. J. A **36**, 243 (2008).

[28] S. Pascu, Gh. Căta-Danil, D. Bucurescu, N. Mărginean, C. Müller, N. V. Zamfir, G. Graw, A. Gollwitzer, D. Hofer, and B. D. Valnion, Phys. Rev. C **81**, 014304 (2010).

[29] J. B. Gupta and M. Saxena, Phys. Rev. C **91**, 054312 (2015).

[30] A. J. Mitchell *et al.*, Phys. Rev. C **93**, 014306 (2016).

[31] N. V. Zamfir, W. T. Chou, and R. F. Casten, Phys. Rev. C **57**, 427 (1998).

[32] P. O. Lipas, P. von Brentano, and A. Gelber, Rep. Prog. Phys. **53**, 1355 (1990).

[33] H. Maser, N. Pietralla, P. von Brentano, R.-D. Herzberg, U. Kneissl, J. Margraf, H. H. Pitz, and A. Zilges, Phys. Rev. C **54**, R2129 (1996).

[34] A. Giannatiempo, A. Nannini, P. Sona, and D. Cutoiu, Phys. Rev. C **52**, 2969 (1995).

[35] A. Giannatiempo, Phys. Rev. C **98**, 034305 (2018).

[36] A. A. Sonzogni, Nucl. Data Sheets **103**, 1 (2004).

[37] Yu. Khazov, A. A. Rodionov, S. Sakharov, and B. Singh, Nucl. Data Sheets **104**, 497 (2005).

[38] H. Naïdja, F. Nowacki, B. Bounthong, M. Czerwiński, T. Rząca-Urban, T. Rogiński, W. Urban, J. Wiśniewski, K. Sieja, A. G. Smith, J. F. Smith, G. S. Simpson, I. Ahmad, and J. P. Greene, Phys. Rev. C **95**, 064303 (2017).

[39] NNDC data base, http://nndc.bnl.gov.

[40] I. Talmi, *Simple Models of Complex Nuclei* (Harwood Academic, Switzerland, 1993).

[41] O. Scholten, K. Heyde, P. Van Isacker, and T. Otsuka, Phys. Rev. C **32**, 1729 (1985).

[42] I. Talmi, Phys. Lett. B **405**, 1 (1997).

[43] A. Giannatiempo, A. Nannini, and P. Sona, Phys. Rev. C **58**, 3316 (1998).

[44] A. Giannatiempo, A. Nannini, and P. Sona, Phys. Rev. C **58**, 3335 (1998).

[45] D. D. Warner and R. F. Casten, Phys. Rev. Lett. **48**, 1385 (1982).

[46] C. De Coster and K. Heyde, Int. J. Mod. Phys. A **04**, 3665 (1989).

[47] T. Otsuka and N. Yoshida, Program NPBOS Japan Atomic Energy research Institute report JAErI-M85-094, 1985.

[48] F. Iachello, in *Interacting Boson Model in Nuclear Physics*, edited by F. Iachello (Plenum Press, New York, 1979).

[49] T. Tamura, Nucl. Data Sheets **108**, 455 (2007).

[50] S. Pilotte, S. Flibotte, S. Monaro, N. Nadon, D. Prévost, P. Taras, H. R. Andrews, D. Horn, V. P. Janzen, D. C. Radford, D. Ward, J. K. Johansson, J. C. Waddington, T. E. Drake, A. Galindo-Uribarri, and R. Wyss, Nucl. Phys. A **514**, 545 (1990).

[51] A. A. Sonzogni, Nucl. Data Sheets **93**, 599 (2001).

[52] D. C. Biswas, A. G. Smith, R. M. Wall, D. Patel, G. S. Simpson, D. M. Cullen, J. L. Durell, S. J. Freeman, J. C. Lisle, J. F. Smith, B. J. Varley, T. Yousef, G. Barreau, M. Petit, Ch. Theisen, E. Bouchez, M. Houry, R. Lucas, B. Cahan, A. Le Coguie, B. J. P. Gall, O. Dorvaux, and N. Schulz, Phys. Rev. C **71**, 011301(R) (2005).

[53] B. Bucher *et al.*, Phys. Rev. Lett. **116**, 112503 (2016).

[54] Yu. Khazov, A. Rodionov, and G. Shulyak, Nucl. Data Sheets **136**, 163 (2016).

[55] B. Bucher, S. Zhu, C. Y. Wu, R. V. F. Janssens, R. N. Bernard, L. M. Robledo, T. R. Rodríguez, D. Cline, A. B. Hayes, A. D. Ayangeakaa, M. Q. Buckner, C. M. Campbell, M. P. Carpenter, J. A. Clark, H. L. Crawford, H. M. David, C. Dickerson, J.

Harker, C. R. Hoffman, B. P. Kay, F. G. Kondev, T. Lauritsen, A. O. Macchiavelli, R. C. Pardo, G. Savard, D. Seweryniak, and R. Vondrasek, Phys. Rev. Lett. **118**, 152504 (2017).

[56] R. Lică *et al.*, Phys. Rev. C **97**, 024305 (2018).

[57] P. G. Bizzeti *et al.*, Phys. Rev. C **82**, 054311 (2010).

[58] P. Petkov, A. Dewald, and W. Andrejtscheff, Phys. Rev. C **51**, 2511 (1995).

[59] A. Dewald, D. Weil, R. Krücken, R. Kühn, R. Peusquens, H. Tiesler, O. Vogel, K. O. Zell, P. von Brentano, D. Bazzacco, C. Rossi-Alvarez, P. Pavan, D. DeAcuña, G. De Angelis, and M. De Poli, Phys. Rev. C **54**, R2119 (1996).

[60] G. Seiler-Clark, D. Husar, R. Novotny, H. Gräf, and D. Pelte, Phys. Lett. B **80**, 345 (1979).

[61] K. Schiffer, S. Harissopulos, A. Dewald, A. Gelberg, K. O. Zell, P. von Brentano, P. J. Nolan, A. Kirwan, D. J. G. Love, D. J. Thornley, and P. J. Bishop, J. Phys. G **15**, L85 (1989).

[62] G. S. Li, Z. Y. Dai, X. A. Liu, L. K. Zhang, S. X. Wen, G. J. Yuan, X. G. Wu, P. K. Weng, S. G. Li, and C. X. Yang, Eur. Phys. J. A **1**, 379 (1998).

[63] K. S. Krane and R. M. Steffen, Phys. Rev. C **2**, 724 (1970).

[64] H. Frauenfelder and R. M. Steffen, in *Alpha-, Beta-, and Gamma-Bay Spectroscopy*, edited by K. Siegbahn (North-Holland Publishing Company, Amsterdam, 1965), p. 997.

[65] D. S. Brenner, R. B. Cakirli, and R. F. Casten, Phys. Rev. C **73**, 034315 (2006).

[66] R. B. Cakirly and R. F. Casten, Phys. Rev. Lett. **96**, 132501 (2006).

[67] R. F. Casten, *Nuclear Structure from a Simple Perspective* (Oxford University Press, Oxford, 1990).

[68] L. Wilets and M. Jean, Phys. Rev. **102**, 788 (1956).

[69] A. S. Davydov and A. A. Chaban, Nucl. Phys. **20**, 499 (1960).

[70] A. S. Davydov and G. F. Filippov, Nucl. Phys. **8**, 237 (1958).

[71] R. F. Casten, P. von Brentano, K. Heyde, P. Van Isacker, and J. Jolie, Nucl. Phys. A **439**, 289 (1985).

[72] B. Sorgunlu and P. Van Isacker, Nucl. Phys. A **808**, 27 (2008).

[73] N. V. Zamfir and R. F. Casten, Phys. Lett. B **260**, 265 (1991).

[74] P. Van Isacker, K. Heyde, J. Jolie, and A. Sevrin, Ann. Phys. **171**, 253 (1986).